

Samuel Johnson

7/25/68

MECHANICAL BEHAVIOR OF THERMOMECHANICALLY  
TREATED X-60 STEEL

A THESIS

Presented to

The Faculty of the Division of Graduate  
Studies and Research

by

Samuel Alfred Andrew

In Partial Fulfillment

of the Requirements for the Degree

Master of Science


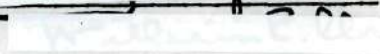
in Mechanical Engineering

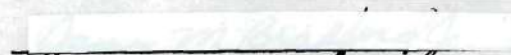


Georgia Institute of Technology

June 1972

MECHANICAL BEHAVIOR OF THERMOMECHANICALLY  
TREATED X-60 STEEL

Approved:

  
Chairman 

  
  
  
Date approved by Chairman: 5-26-72

## ACKNOWLEDGMENTS

The author would like to express his gratefulness and thanks to the many individuals who made this thesis possible. Much appreciation is owed to the Republic Steel Corporation whose personnel made possible the fabrication program. Particular thanks are due Dr. A. B. Blocksidge, Jr., Assistant Director of Research, Dr. C. B. Griffith, Chief, Metallurgical Development Section, and Mr. U. B. Gammon.

The author would especially like to express his gratitude to the late Dr. W. R. Clough who initially suggested this investigation. Although his illness hindered him, Dr. Clough's assistance and suggestions were indispensable to this work. The author is grateful to Dr. S. P. Kezios who offered his assistance with the demise of Dr. Clough. Special thanks go to Dr. J. M. Bradford, Dr. E. E. Underwood, and Dr. J. M. Anderson who gave advice and help on several occasions. Dr. N. N. Engel of the School of Chemical Engineering and his assistants made available the metallograph for the necessary metallographic work. Messrs. R. G. Grim, B. L. Wallace, and J. W. Davis gave valuable advice when test specimens were prepared in the machine shop.

This thesis is dedicated to my mother whose love and understanding greatly encouraged my continuing education.

## TABLE OF CONTENTS

	Page
ACKNOWLEDGMENTS . . . . .	ii
LIST OF TABLES . . . . .	v
LIST OF ILLUSTRATIONS . . . . .	vi
SUMMARY . . . . .	ix
Chapter	
I. INTRODUCTION . . . . .	1
General Background	
Thesis Objective	
Thermomechanical Treatments of Steels	
High Strength, Low Alloy Steels	
General Microstructure Considerations	
Stress-Strain Relationship	
Republic X-60 Steel	
II. MATERIAL, FABRICATION, AND SPECIMEN PREPARATION . . .	21
X-60 Steel	
The Thermomechanical Treatment Program	
Preparation of Test Specimens	
III. EXPERIMENTAL PROCEDURES . . . . .	31
Tensile Tests	
Charpy Impact Tests	
Hardness Tests	
Metallographic Analysis	
IV. RESULTS . . . . .	41
Mechanical Properties	
Metallographic Analysis	
V. DISCUSSION . . . . .	56
General	
Lower Yield Strength	

## TABLE OF CONTENTS (Concluded)

Chapter	Page
V. DISCUSSION (Continued)	
Ultimate Tensile Strength	
Hall-Petch Equation	
Strain Hardening Exponent	
Strength Coefficient	
Per Cent Elongation (Ductility)	
V-Notch Charpy Transition Temperature	
Ferrite Orientation Factor	
Ferrite Mean Intercept Diameter	
Comparison of Results	
Photomicrographs	
VI. CONCLUSIONS . . . . .	94
BIBLIOGRAPHY . . . . .	96

## LIST OF TABLES

Table	Page
1. Designation of Fabrication Samples . . . . .	26
2. Tensile Test Results Related to Yielding, Hot Work Samples . . . . .	43
3. Tensile Test Results Related to Yielding, Cold Work-Hot Work Samples . . . . .	44
4. Tensile Test Results Related to Necking, Hot Work Samples . . . . .	45
5. Tensile Test Results Related to Necking, Cold Work-Hot Work Samples . . . . .	46
6. Tensile Test Results Related to Fracture, Hot Work Samples . . . . .	47
7. Tensile Test Results Related to Fracture, Cold Work-Hot Work Samples . . . . .	48
8. Charpy Test Results, Hot Work Samples . . . . .	49
9. Charpy Test Results, Cold Work-Hot Work Samples . . . . .	51
10. V-Notch Charpy Transition Temperature . . . . .	53
11. Hardness Test Results, Hot Work Samples . . . . .	54
12. Hardness Test Results, Cold Work-Hot Work Samples . . . . .	54
13. Optical Metallographic Results, Hot Work Samples . . . . .	55
14. Optical Metallographic Results, Cold Work- Hot Work Samples . . . . .	55

## LIST OF ILLUSTRATIONS

Figure	Page
1. Location of Test Samples Relative to Fabricated Plate . . . . .	27
2. Test Specimen Dimensions . . . . .	29
3. Lower Yield Strength as a Function of Fabrication Temperature, Hot Work Specimens . . . . .	57
4. Lower Yield Strength as a Function of Fabrication Temperature, Cold Work- Hot Work Specimens . . . . .	58
5. Ultimate Tensile Strength as a Function of Fabrication Temperature, Hot Work Specimens . . . . .	61
6. Ultimate Tensile Strength as a Function of Fabrication Temperature, Cold Work-Hot Work Specimens . . . . .	62
7. Applicability of the Hall-Petch Equation, Hot Work Longitudinal Specimens . . . . .	63
8. Applicability of the Hall-Petch Equation, Cold Work-Hot Work Longitudinal Specimens . . . . .	65
9. Strain Hardening Exponent as a Function of Fabrication Temperature, Hot Work Specimens . . . . .	66
10. Strain Hardening Exponent as a Function of Fabrication Temperature, Cold Work- Hot Work Specimens . . . . .	67
11. Strength Coefficient as a Function of Fabrication Temperature, Hot Work Specimens . . . . .	71
12. Strength Coefficient as a Function of Fabrication Temperature, Cold Work- Hot Work Specimens . . . . .	72

## LIST OF ILLUSTRATIONS (Continued)

Figure	Page
13. Per Cent Elongation as a Function of Fabrication Temperature, Hot Work Specimens . . . . .	74
14. Per Cent Elongation as a Function of Fabrication Temperature, Cold Work- Hot Work Specimens . . . . .	75
15. V-Notch Charpy Transition Temperature as a Function of Fabrication Temperature . . . . .	77
16. Ferrite Orientation Factor as a Function of Fabrication Temperature . . . . .	79
17. Ferrite Mean Intercept Diameter (d) as a Function of Fabrication Temperature . . . . .	81
18. Comparison of Lower Yield Strengths and Ultimate Tensile Strengths . . . . .	83
(a) Lower Yield Strength	
(b) Ultimate Tensile Strength	
19. Comparison of Strain Hardening Exponents (n) . . . . .	84
20. Comparison of Strength Coefficients (K) . . . . .	85
21. Comparison of Charpy Transition Temperatures and Ductilities (Total Per Cent Elongation) . . . . .	86
(a) Charpy Transition Temperature	
(b) Elongation	
22. Photomicrograph of the Hot Work Material at 950°F Fabrication, Magnification 400x . . . . .	89
23. Photomicrograph of the Hot Work Material at 1400°F Fabrication, Magnification 400x . . . . .	90

## LIST OF ILLUSTRATIONS (Concluded)

Figure	Page
24. Photomicrograph of the Hot Work Material at 1550 <sup>o</sup> F Fabrication, Magnification 400x . . . . .	91
25. Photomicrograph of the Hot Work Material at 1700 <sup>o</sup> F Fabrication, Magnification 400x . . . . .	92
26. Photomicrograph of the Hot Work Material at 2000 <sup>o</sup> F Fabrication Magnification 400x . . . . .	93

## SUMMARY

Research recently completed by Y. M. Ebadi (single addition "Mn" high strength, low alloy steel) and by M. R. Pereyra (triple addition "Mn, V, Cu" high strength, low alloy steel) have shown that some mechanical properties of structural steels are strongly influenced by changes of fabrication temperatures at the hot mill. The objective of this investigation is to determine if equivalent behavior is experienced in a double addition (Mn, Cb) high strength, low alloy steel designated by the Republic Steel Corporation as X-60 steel. Plate samples in an initial hot worked condition were hot rolled at several temperatures within the single phase austenitic field, at several temperatures within the critical range, and at several temperatures below the eutectoid temperature. Hot rolling was also performed at the above temperatures on plate samples that were initially cold worked.

It was concluded from the calculated results that hot rolling (high temperature thermomechanical treatment - HTTMT) at 1550°F gave the optimum combination of mechanical properties of X-60 steel. Ductility, lower yield strength, the strain hardening exponent, and the Charpy transition temperature were all considerably improved when compared to X-60 steel in the regular mill condition. It was also concluded that preliminary thermomechanical treatment (PTMT) was not beneficial to yielding an optimum combination of mechanical properties.

The fabrication temperature of 1550°F was most likely near the austenite-ferrite transformation temperature, and the resulting fine and equiaxed ferrite grain structure gave increased toughness and ductility. Fabrication at temperatures above 1400°F resulted in property variations controlled by ferrite grain size, and the Hall-Petch relationship seemed to be applicable. Fabrication below 1400°F introduced hardening effects, possibly complicated by strain aging.

## CHAPTER I

### INTRODUCTION

#### General Background

Within recent years, new classes of structural steels, which are designated as "high strength, low alloy steels" (HSLA), have been introduced. These steels differ from the usual plain carbon structural steels which contain only certain amounts of carbon, manganese, phosphorus, sulfur, and silicon. The HSLA structural steels contain small and economical alloy additions, such as 0.05 w/o V or 0.05 w/o Cb, which greatly increase resistance to deformation as measured by yield strength, flow stress, or ultimate strength. Even with these alloy additions, structural steels, which are used for beams, channels, plates, etc., will still maintain good ductility characteristics, low ductile-brittle transition temperatures, and good weldability.

Structural steels, whether plain carbon or HSLA, are usually utilized in the condition resulting from "hot worked" fabrication (1700 to 2100°F). For such steels, the temperature range is well into the single phase austenitic region. Steels of a given composition, which are produced by a given combination of thermo-mechanical processes, will then possess a given set of mechanical properties which will show little variation from heat to heat. The engineer therefore has available a "standard" set of properties for

each structural steel.

### Thesis Objective

The objective of this thesis was to determine experimentally for HSLA steels a preferable fabrication temperature or range of temperatures which would yield an optimum combination of mechanical properties instead of the "standard" properties. The HSLA steel selected for this investigation was Republic Steel's X-60 double alloy addition steel which contains low level alloy additions of manganese and columbium. A single low alloy addition (Mn) steel (X-52) and a triple low alloy addition (Mn,V,Cu) steel (A-441) have already been investigated in other related thesis work.

To accomplish the objective of the research, an experimental fabrication program was made possible by the acknowledged personnel of the Republic Steel Research Center in Cleveland, Ohio. The X-60 steel, which had two different initial conditions (mill and cold worked), was fabricated at several temperatures within the single phase austenitic region (above the  $A_3$  line), at temperatures within the two phase austenite-ferrite range (between the  $A_1$  and  $A_3$  lines), and at several temperatures within the two phase ferrite-pearlite range (below the eutectoid temperature). The temperatures and rolling reductions used in the experimental fabrication program were specified on the basis of experience and theory.

The properties that were considered were yield strength, ultimate tensile strength, uniform elongation, per cent reduction of area, per cent elongation, strain hardening exponent, strength

coefficient and ductile-brittle transition temperatures. The effects of fabrication variables on microstructures were investigated also.

### Thermomechanical Treatments of Steels

#### General

Hardening or strengthening of materials can be accomplished by the pertinent metallurgical mechanisms which are carried out either simultaneously with fabrication at the hot mill or immediately following hot mill fabrication. This type of treatment has received considerable research and development within recent years. Some of these thermomechanical treatment developments have been reduced to commercial practice and are now used in the steel industry in the United States, Great Britain, and the Soviet Union.

High Temperature Thermomechanical Treatment (HTTMT). Work hardening may be accomplished simultaneously with recrystallization, even if the steel hot fabrication is done in the austenite single phase region. This is known as the high temperature thermomechanical treatment (HTTMT) process. The results of such work hardening treatment include increases in values of yield strength, ultimate tensile strength, ductility, and fatigue properties when such values are compared with properties obtained with more conventional heat treatments. The degree of change of properties depends on the specific alloy and on the variation of processing parameters.

In his recent survey of thermomechanical treatments as accomplished in the Soviet Union, Koppenaal (1) has concluded that

there is a formation of carbides during HTMT when precipitation hardening steels are fabricated. The solid solubility of carbon in austenite is thought to be considerably reduced with simultaneous plastic deformation, resulting in carbide formation during HTMT. The carbides will reenter solid solution as soon as the deformation is completed unless the steel is quenched. From an industrial viewpoint, HTMT is important since the deformation is performed at temperatures compatible with existing fabrication facilities. In many cases, recrystallization cannot be completely avoided during HTMT. Thus steels with slow recrystallization kinetics, such as tool steels, are considered to be (2) particularly applicable for HTMT.

An effective HTMT has been described by Ivanova and Gordienko (3). Steel was heated well into the austenite region ( $1150-1200^{\circ}\text{C}$ ), cooled to a temperature slightly above the  $A_3$  line, and then given 25-30 per cent plastic deformation. After the thermomechanical treatment, the steel was immediately water quenched and tempered in the low temperature range from 100 to  $200^{\circ}\text{C}$ . Yield strength increases were of the order of 10 to 20 per cent as compared with the same steels which were given the same thermal treatments without the accompanying plastic deformation. The plastic deformation was considered to be responsible for the development of a very fine microstructure. When deformed at temperatures just above the  $A_3$  line instead of at higher temperatures, the rate of recrystallization of austenite is comparatively slow. Quenching was done to prevent recrystallization and to promote the martensite

reaction with the applicable steels.

Low Temperature Thermomechanical Treatment (LTTMT). This process designated as LTTMT is also referred to as "ausforming". Steels capable of forming martensite are used, and the process consists of deforming the steel while its temperature is between the recrystallization range and the martensite start  $M_s$  temperature. The LTTMT process can give high increases in yield strength as well as increased ductility. High alloy steels are most suitable for LTTMT since there is a sufficiently wide metastable austenite bay in the time-temperature cooling diagram to allow time for fabrication to be accomplished. During the LTTMT process, a number of structural changes may take place. Since the deformation temperature is below the solution temperature for most of the carbides, deformation will be performed simultaneously with carbide precipitation. Another feature of LTTMT is that during the austenite-martensite transformation, the high dislocation density of the deformed austenite is retained by the martensite, resulting in strengthening. A typical LTTMT is described in detail in the Russian translation (3).

Controlled Cooling. The combination of accelerated cooling from hot mill temperatures and control of coiling temperatures has received attention when thin strip products are considered. This process would not apply to thick plates since thick plate is difficult to cool uniformly and since plate is usually not coiled.

The influence of various schedules after the hot rolling of 1/4 inch plate of structural steels modified with columbium,

molybdenum, and boron has been recently reported by Cryderman, Coldren, Bell, and Grozier (4). Strength increases resulting from these treatments were associated with grain refinement of the ferrite. Previous investigations (5) had concluded that accelerated cooling did not effectively suppress the recrystallization of austenite in carbon steel. But in precipitation hardening steels which contain such alloy additions as columbium and vanadium, the austenite recrystallization completion is retarded.

The controlled cooling of steel strip after coiling can also play an important part in the control of properties. If the temperature at the coil is sufficiently high and if the austenite decomposition transformation has not been completed on the run-out table, then the transformation will be continued in the coil, and precipitation hardening will take place in applicable alloyed steels.

Isoforming. Isoforming consists of fabrication performed simultaneously with the austenite-pearlite reaction. A result is the obtaining of a very fine subgrain structure in the ferrite. Also partial or complete spheroidization may take place (6). It has been found in several alloy steels, that only small improvements in ultimate and yield strengths were obtained by isoforming. However, there were improvements in toughness as measured by decreases in the notch-brittle-ductile transition temperature.

Preliminary Thermomechanical Treatment (PTMT). The PTMT process involves performing plastic deformation before austenization. It has been established (1) that there are strengthening effects if (a) steels are cold worked before austenization, and (b) if the

cold worked steels are rapidly heated to the austenization temperature. It appears that some of the dislocations introduced by preliminary cold work are retained during thermal processing.

#### Other Considerations

Many grades of structural steels are utilized for engineering applications when these steels are still in the condition derived from the hot mill. Rolling to a lower than normal finishing temperature at the hot mill can lower the impact transition temperature (7,8,9). This is probably due to the increase of cooling rate and to the correspondingly reduced ferrite grain size. Heat transfer considerations dictate that under identical thermomechanical treatments, thick plates cool more slowly than thin plates and therefore thick plates will have larger ferrite grain sizes and higher ductile-brittle transition temperatures (10). Post rolling normalizing treatments are sometimes given directly after hot rolling to improve the properties of rolled plate (11).

Deformation accomplished in the plastic region will promote strengthening effects of an alloy steel through strain hardening. It is not uncommon for the yield strength (flow stress) of steels to be doubled or tripled or to be further increased by cold work. Cold work deformation can also raise the Charpy ductile-brittle transition temperature.

The processes of HTMT and LTMT have been successfully combined into one processing schedule (1) which has been referred to as combined thermomechanical treatment or CTMT. Encouraging

results have been obtained with 0.3 - 0.4 w/o C steels containing W, V, Ni, and/or Mo additions. Yield strength increases of 35 to 45 per cent and ultimate tensile strength increases of 10 to 30 per cent have resulted from application of CTMT; these measures of strength are compared with those resulting from conventional hot rolling (1).

### High Strength, Low Alloy Steels

#### Some Characteristics of HSLA Steels

The alloy additions of HSLA steels have considerably modified the properties of hot rolled carbon steels in that they promote a precipitation hardening capability, finer and stronger ferritic-pearlitic structures (increased hardenability), better ferrite strength, and improved corrosion resistance (5,12,13).

The levels of alloy additions that can be made to improve the strength of HSLA steels are usually limited by weldability considerations. Since structural steels are often welded, low levels of alloy additions such as vanadium and columbium have been found to promote increased strength through precipitation hardening mechanisms while maintaining weldability. Columbium has been found to be a useful precipitation hardening strengthening agent for the practical reason that it can be recovered easily from killed or semikilled steels. Columbium carbide and nitride have complete solid solubility in steels such that the compound found in commercial columbium containing HSLA steels is referred to as a carbonitride. A steel containing 0.2 w/o C, 0.1 w/o N, and 0.03 w/o Cb needs to be heated

to 2100°F before columbium carbonitrides go into solid solution (14,15). The soaking pit temperature at or above 2300°F should insure solution of the columbium carbonitrides in HSLA steels. During (16) and after (17) the transformation to ferrite on cooling, the columbium remaining in solid solution causes hardening by the precipitation of very fine carbonitride particles, and thus the steel is strengthened. Raising the strength of steels by columbium additions results in a loss of toughness, but this can be often offset by reducing the ferrite grain size by process control. The solubility and the precipitation hardening powers of vanadium carbide and vanadium nitride are different from those of corresponding columbium compounds. In HSLA steels that contain about 0.2 w/o C, 0.01 w/o N, and 0.05 w/o V, the vanadium carbide and nitride go into solid solution at temperatures at or above 1800°F (18,19) which is lower than the previously given solution temperature for columbium carbonitride.

Hardenability is increased in steels with the presence of such alloy additions as carbon, manganese, nitrogen, silicon, nickel, chromium, molybdenum, copper, columbium, and vanadium; all of which are in solid solution in the austenite phase. The term "hardenability" refers to the phenomena of retardation of the transformation of austenite which causes a decrease in the formation temperature of ferrite during continuous cooling. There is then a decrease in ferrite grain size causing a decrease in volume per cent of ferrite and thus resulting in an increase in pearlite. Hardenability creates a finer and stronger ferritic-pearlitic structure.

Alloying additions give better ferrite strength in ferrite steels by substitutional solid solution hardening mechanisms. Copper and phosphorus are widely used as solution strengthening additions. Manganese and nickel additions improve toughness as well as raising strength.

Atmospheric corrosion resistance of HSLA steels are noticeably improved by the addition of such elements as chromium, copper, phosphorus, silicon, and nickel (20). As little as 0.2 w/o Cu is sufficient to double the atmospheric corrosion resistance of carbon steels, but increased copper concentration beyond this level is less effective. These alloy additions improve paint life for these steels, and in many cases these structural steels are used in the unpainted condition.

#### Additional Considerations of HSLA Steels

Irving (21) has published an excellent article which reviews the development of high strength, low alloy steels (HSLA steels). This same reference contains also much technical information pertaining to fabrication procedures and applications for these steels. The technical literature dealing with the various columbium and vanadium effects of HSLA steels has become extensive.

One important effect of columbium additions is that the recrystallization temperature of austenite is raised, and the rate of recrystallization of austenite is retarded. Effects on the recrystallization kinetics are due to the fact that columbium carbonitride can be formed in austenite (17). Recent German work (22) has demonstrated that precipitation can be completed in just

four minutes at 1650°F, and it is also clear that the rate of precipitation is accelerated by simultaneous plastic deformation. Recent experimentation (23) has shown that decreasing the finishing temperature at the hot mill results in increased columbium carbonitride precipitation in austenite so that less columbium remains in solution to influence later processes such as precipitation hardening of the subsequently formed ferrite. The influence of columbium on the rate of transformation has received relatively little attention in the technical literature, although it has been shown (24) that columbium has a significant retarding effect on the transformation to ferrite and pearlite but little to no effect on bainite formation.

Similar properties and responses are obtainable in vanadium and columbium containing steels by means of process control, and no distinction is made in some ASTM or API specifications for steels containing these additions. For example, ASTM A572 specifies 0.005 - 0.11 w/o V or 0.004 - 0.06 w/o Cb when added singly, or a maximum of 0.05 w/o Cb when added in combination with 0.01 - 0.11 w/o V. Pipe made to API designation 5LX-Grade X-60 can contain minimums of 0.005 w/o Cb, 0.02 w/o V, and 0.03 w/o Ti, either alone or in combination. Unless the particular addition element is specified by the customer, the choice of additions is at the discretion of the producer.

Such alloy additions to steel as manganese, aluminum, and vanadium lower the tendencies for strain age embrittlement. Manganese retards the precipitation of nitrides, and aluminum and vanadium

getter the nitrogen in the form of vanadium carbides or nitrides during normalizing or hot rolling. Silicon is also beneficial in this respect since it is an effective deoxidizer and leaves aluminum free to getter the nitrogen.

Irani, Dulieu, and Tither (25) have recently summarized the role of copper as an addition to low alloy steels. One effect regarding corrosion has been mentioned above. A useful strengthening effect in steel may be obtained by tempering when copper is present in amounts between 0.60 and 1.50 w/o. An additional strengthening response is obtained when copper is added in combination with columbium or vanadium.

In addition to the papers above, the research papers of Stephenson, Karchner, and Stark (26) dealing with strengthening mechanisms in Mn-V-N steels and of W. B. Morrison (27) dealing with the influence of small columbium additions on the properties of various carbon-manganese steels are regarded as technical milestones.

#### General Microstructure Considerations

If the grain size is the only variable in different samples of a specific material, the grain size will become a factor in altering the values of the mechanical properties in that material. For example, values of yield strength, ultimate tensile strength, and hardness will all increase with decreasing grain size. Grain size would be an important factor when measuring properties which are characteristic of early plastic deformation since grain boundary barriers to dislocation motion are most effective at this stage.

For example yield strength would be more dependent on grain size than would be ultimate tensile strength. Ultimate tensile strength (31) would be more controlled by complex dislocation interactions taking place within the pearlite and thus it would be more dependent on volume fraction of pearlite.

Hall(28) and Petch (29) derived from considerations of dislocation theory a relationship between yield strength,  $\sigma_y$ , and the grain size (grain diameter,  $d$ ). The relationship known as the Hall-Petch equation is as follows:

$$\sigma_y = \sigma_i + K_y d^{-\frac{1}{2}} \quad (1)$$

where  $\sigma_i$  = the friction stress; that is the stress which opposes the motion of dislocations

$K_y$  = the strength coefficient; a measure of the extent to which dislocations are piled up at a barrier, as against a given boundary

The strength coefficient,  $K_y$ , which is essentially independent of temperature, is evaluated from the slope of the plot of the equation. The value of the intercept on the plot,  $\sigma_i$ , is a measure of the stress required to drive a dislocation against the resistance offered by impurities, precipitate particles, subgrain boundaries, and other obstacles to dislocation motion. The friction stress value depends on composition, metallurgical condition, and temperature, thus indicating the necessity of applying equation (1) only for a given

metal with samples in identical condition except for grain size.

The Hall-Petch equation has been applied to and verified for a wide variety of steels and many nonferrous alloys.

Many alloy additions which make up low carbon steels result in some solid solution hardening of the ferrite and thus raise the values of the friction stress  $\sigma_1$ . These alloy additions may also result in the austenite-ferrite transformation taking place at lower temperatures, thus producing smaller ferrite grain size. Both of these effects will raise the yield strength as dictated by the Hall-Petch equation. When these two effects are the only ones of importance for a steel being considered, quantitative metallographic procedures and multiple regression analysis done with computers have allowed these two effects to be separated. It is then possible to express the Hall-Petch relationship in terms of chemical compositions (30) as in the following general form:

$$\sigma_y = C_1 + C_2 d^{-\frac{1}{2}} + \sum_{i=1}^n \alpha_i \quad (2)$$

The strength increase term,  $\alpha_i$ , is in units of psi per weight per cent of alloy in solid solution in the ferrite. The summation is taken over the N alloy additions which are in solution in the ferrite. It should be noted that equations (1) and (2) do not take into account such metallurgical phenomena as cold working, aging, or precipitation effects, all of which influence the values of the

friction stress  $\sigma_i$ .

Pickering's group (30,31) accomplished the original work by computer regression in the development of relationships such as equation (2). Variables such as grain size (ferrite), volume fraction of pearlite, solution hardening effects, and cooling transformation effects were considered for alloy additions such as manganese and silicon which were used in a wide range of structural steel compositions. The result of the yield strength regression analysis was:

$$\sigma_y(\text{PSI}) = 15,000 + 4,720(\text{w/o Mn}) + 12,150(\text{w/o Si}) \quad (3)$$

$$+ 507 d^{-\frac{1}{2}}$$

Various modifications of Pickering's formulation (equation (3)) have been developed which take into account mill fabrication conditions, different alloy additions, and weight per cent of free nitrogen (32,33, 34).

Some investigators, including Pickering and Gladman (30), have concluded that for the case for plain carbon steels with carbon contents below 0.2 w/o, the value of  $\sigma_y$  is independent of the volume fraction of pearlite in the steel, allowing for the development of such relationships as equation (3). It has been reasoned that although the pearlite patches are comparatively hard as opposed to ferrite grains, they are so widely dispersed in the ferrite

matrix that the ferrite can deform around these patches without difficulty. However, some investigators believe that the effects of pearlite on yield strength values may be significant. Korchynsky (35) and his associates at the Graham Research Laboratories of Jones and Laughlin Steel Corporation developed the following modification to Pickering's formulation which considers the volume fraction (v/o) of pearlite:

$$\begin{aligned}\sigma_y = & 13,000 + 3,500 \text{ (w/o Mn)} + 9,000 \text{ (w/o Si)} \quad (4) \\ & + 4,000 \text{ (w/o Ni)} + 99 \text{ (v/o pearlite)} \\ & + 591 d^{-\frac{1}{2}}\end{aligned}$$

After plastic flow has been well initiated in a tensile test for example, any existing pearlite patches are closer together and can then exert possible significant plastic constraint factors upon further deformation of ferrite. This would lead to an increase of strain hardening rate, and thus an expected result would be that the ultimate tensile strength of annealed carbon steels would be increased by the presence of pearlite. It has been already pointed out that the ultimate tensile strength (UTS) would be influenced by the volume fraction of pearlite to a greater extent than would be the yield strength. Pickering and his group (30,31) developed the formulation:

$$\begin{aligned} \text{UTS (PSI)} = & 42,700 + 3,990 (\text{w/o Mn}) + 12,000(\text{w/o Si}) \quad (5) \\ & + d^{-\frac{1}{2}} + 560 (\text{v/o pearlite}) \end{aligned}$$

Other formulations for ultimate tensile strength have been developed for steels at different fabrication conditions and with different alloy additions (32,33).

Pickering and his associates (30,31) also developed formulations for approximating tensile ductility (% RA, per cent reduction of area) and the Charpy impact temperature, ITT ( $^{\circ}\text{C}$ ):

$$\% \text{ RA} = 78.5 + 5.39 (\text{w/o Mn}) - 0.53 (\text{v/o pearlite}) \quad (6)$$

$$- 8399 d$$

$$\text{ITT } (^{\circ}\text{C}) = 63 + 44.1 (\text{w/o Si}) - 258 (\text{w/o Al}) \quad (7)$$

$$+ 2.2 (\text{w/o pearlite}) - 2.3 d^{-\frac{1}{2}}$$

It is emphasized again that all the equations mentioned above were developed for metallurgically simple steels, such as normalized plain carbon structural steels. These equations do not account for complications that would result because of phenomena such as cold work, precipitation, or strain aging which would influence  $\sigma_1$  values.

### Stress-Strain Relationship

The common engineering tensile stress-strain curve is really not suitable for describing the plastic behavior and work hardening characteristics of metals and alloys. Superior description of work hardening is obtained when the tensile true stress-true strain curve is considered. The true stress-true strain behavior in tension can be described by the following formulation:

$$\bar{\sigma} = K \bar{\epsilon}^n \quad (8)$$

where  $\bar{\sigma}$  = the true stress in psi

$\bar{\epsilon}$  = the true strain

K = the strength coefficient in psi

n = the strain hardening exponent

Thus there is implied a linear relationship between  $\log \bar{\sigma}$  and  $\log \bar{\epsilon}$ , with the value of the slope of such a plot (when  $\log \bar{\sigma}$  is plotted as the ordinate) being the value of the strain hardening exponent n.

The value of K, which is the strength coefficient, is the value of true stress at the plot intercept where the true strain has a value of one. If a material is found to obey the relationship given by equation (8), Considère's second construction (37) will then show that it is necessary for the true strain at the instant of necking to have a value equal to that of n. Thus the strain hardening exponent is a measure of the rate of work hardening of the material being considered. A low slope value for the  $\log \bar{\sigma} - \log \bar{\epsilon}$  plot

indicates a low value of work hardening (change of flow stress with change of plastic deformation), and a low value of true elongation before necking commences. A high slope value corresponds to rapid work hardening.

Many of the experimentally determined plots of  $\log \bar{\sigma}$  against  $\log \bar{\epsilon}$  for low alloy steels do not show actual linearity in the plastic range, and as a result, a number of modifications of equation (8) have been proposed. A new relationship proposed by Gladman, Holmes, and Pickering (38) has been found to give excellent agreement with much experimental data obtained in tension with low carbon steel specimens:

$$\bar{\sigma} = a + b \ln \bar{\epsilon} + c \bar{\epsilon} \quad (9)$$

where  $a$ ,  $b$ , and  $c$  are constants.

The literature survey resulted in the finding of one reference which considered the strain hardening exponent  $n$  to be a function of grain size. Morrison (36) obtained:

$$n = \frac{5}{10 + d^{-\frac{1}{2}}} \quad (10)$$

This developed relationship was considered to be an approximation for steels which were metallurgically simple and in soft conditions.

### Republic X-60 Steel

Republic X-60 steel is a double low alloy grade of HSLA containing manganese and columbium. The chemical composition of the X-60 steel used in the fabrication program of this thesis was 0.25 w/o C, 1.10 w/o Mn, 0.017 w/o P, 0.017 w/o S, 0.027 w/o Si, 0.07 w/o Cu, 0.04 w/o Ni, 0.02 w/o Cr, 0.011 w/o Sn, 0.01 w/o Mo, and 0.023 w/o Cb. The Gadsden, Alabama plant of the Republic Steel Corporation rated this steel as having a yield point of approximately 63,000 psi, an ultimate tensile strength of 87,000 psi, and an elongation of 18.0 per cent tensile elongation in an eight inch gage length.

The advertising literature (39) states that X-60 steel has an excellent combination of strength, weldability, and formability, with outstanding atmospheric corrosion resistance. This steel may be used in the unpainted condition since its corrosion resistance is four to six times the resistance of plain structural carbon steel. The 15 ft.-lb. Charpy V-notch transition temperature is given as  $-15^{\circ}\text{F}$ . The steel can be readily welded by the convential arc, resistance, and gas welding process. Republic X-60 meets or exceeds specifications given by ASTM A242 and A588 for plates, structurals, and bars, and ASTM A606 Type 4 for sheet and strip. The steel is used for barges, dredges, railroad cars, earthmoving equipment, farm machinery, trucks and industrial equipment. It is available as hot rolled plates, hot rolled bars, and hot rolled structural shapes.

## CHAPTER II

### MATERIAL, FABRICATION, AND SPECIMEN PREPARATION

#### X-60 Steel

The steel that is investigated in this thesis is Republic Steel's designated X-60, double addition (Mn, Cb) alloy steel. The steel is classified as a high strength low alloy steel (HSLA) which is a new generation of structural steel. This type of steel was selected for this thesis because there has been relatively little work produced for the literature which offers results of thermo-mechanical research of HSLA class steel. The X-60 steel was one of three HSLA steels which were fabricated and provided by the Republic Steel Corporation. The other two steels were X-52, single addition (Mn) alloy steel and A-441, triple addition (Mn, V, Cu) alloy steel. The X-52 and A-441 steels have already been investigated in thesis work by Mr. Y. M. Ebadi and Mr. M. R. Pereyra, respectively, at the Georgia Institute of Technology.

All of the samples of X-60 steel in this investigation were taken from one plate. The plate was prepared and fabricated at the Republic Steel production facility in Gadsden, Alabama. The rolling schedule of the plate was company confidential, but Republic Steel did reveal that the schedule involved some commercial controlled rolling operations including hot finishing. The plate was given the heat number designation 415855.

### The Thermomechanical Treatment Program

Three of the five thermomechanical treatments previously mentioned were involved in this investigation of X-60 Steel. These treatments were high temperature thermomechanical treatment (HTTMT), isoforming, and preliminary thermomechanical treatment (PTMT). The X-60 steel is a low alloyed steel, and therefore the low temperature thermomechanical treatment (LTTMT) could not be used in the investigation because the isothermal transformation diagram of X-60 steel indicates that metastable austenite decomposition at temperatures below the  $A_1$  line will take place in a very short time. The LTTMT is only suitable for high alloy steels. Since LTTMT was impossible to do on this steel, the combined thermomechanical treatment (CTMT) was automatically impossible also. Controlled cooling and coiling was ruled out since the sample sizes were too big and also since the Republic Steel Research Center did not have the proper facilities.

A fabrication program, which consisted of the above three mentioned thermomechanical treatments, was performed by the Republic Steel Research Center. These treatments involved the following temperatures:

a. High temperature thermomechanical treatment (HTTMT) consists of temperatures where all carbides should be in solution and also of temperatures at which carbide precipitation should be concurrent with fabrication. Nitrides or carbonitrides of columbium may be involved instead of just iron-carbides.

b. Isoforming consists of temperatures where the austenite-pearlite reaction could take place simultaneously with plastic

deformation during the rolling process.

c. Preliminary thermomechanical treatment (PTMT) consists of temperatures which are in accordance with the cold work range. Since half of the samples were cold worked before being hot or warm worked at the mill, this treatment was appropriate.

The fabrication program involved temperatures which may be thought of as being low for thermomechanical treatments. These temperatures were well below the  $A_1$  line. Of interest were the effects of possible cold or warm work and of possible simultaneous aging with deformation.

Twenty plate samples were taken from the X-60 steel plate for use in the thermomechanical treatment program. Each sample plate size was 10 inches in length by 6 inches in width by half inch in thickness. The length direction was in the rolling direction of the original plate (Gadsden produced) and was also used as the rolling direction for all further thermomechanical processing. The sample sizes were compatible to the design of the heating facilities and the rolling mill at the Republic Steel Research Center. All fabrication at the Research Center was performed in one two-high reversing mill with 14 inch diameter rolls of 20 inch effective length at a rolling velocity of 1,000 rpm.

One of the samples was given the number designation "1". This sample was representative of the mill conditioned material as produced in Gadsden.

Ten other samples were cold worked at room temperature by rolling to a preliminary 20 per cent reduction of 0.40 inch

thickness. One of these ten samples was given the number designation "2" and it was representative of the cold worked X-60 steel. The other nine samples were each heated in a furnace for one hour at respective temperatures of 2000, 1850, 1700, 1550, 1400, 1250, 1100, 950, and 800°F. These samples were then removed from the furnace and given another 20 per cent reduction in thickness to 0.32 inch by rolling them in one quick pass through the mill. Some of these preliminary cold worked samples represented materials to be involved in the preliminary thermomechanical treatment program (PTMT) as modified by other subsequent operations. All of these preliminary cold worked samples, including the "2" sample, represent the "cold work-hot work" material.

Each of the remaining nine samples, all still in the mill condition, was also heated in a furnace for one hour at respective temperatures of 2000, 1850, 1700, 1550, 1400, 1250, 1100, 950 and 800°F. These samples were then reduced as rapidly as possible from half inch thickness to 0.32 inch with two passes through the rolling mill, each pass giving a 20 per cent reduction. There was little opportunity for a temperature change between passes. These nine samples will be referred to as the "hot-work" material.

Each sample was cooled from fabrication temperature. Immediately after the rolling operation, each sample, while still at temperature, was placed in a granular material specifically provided for cooling purposes.

Samples "1" and "2" were respectively representative of the mill condition and the 20 per cent cold worked X-60. The rest of the

number designations are summarized in Table 1.

### Preparation of Test Specimens

#### General

All test specimens were prepared in the Material Processing Laboratory of the School of Mechanical Engineering, Georgia Institute of Technology. Assistance and guidance was given by acknowledged machine shop personnel. Care was taken during machining operations of the material to avoid distortion or heating which could alter the mechanical properties.

Approximately one inch of material was removed from each plate sample by a single saw cut made with a power hack-saw. This end piece was discarded because it was thought that the end effects resulting from fabrication and heating would distort any representative mechanical properties in the piece. The rest of the plate was used to prepare Charpy specimens, tensile specimens, and metallographic specimens.

#### Charpy Specimens

A  $2\frac{1}{4}$  inch long piece was cut from each sample plate for preparation of Charpy specimens. This piece, as indicated by Figure 1, was cut in a single operation with the power hack-saw. This plate section was surface ground to Charpy specimen length (55 mm) by a Blohm-Simplex 5 surface grinder with a 12 inch diameter wheel. The plate section was also ground to 0.263 inch thickness by the same grinding unit. This thickness was made two-thirds of the thickness of a "standard" Charpy specimen (10 mm) because

Table 1. Designation of Fabrication Samples

Furnace Temperature °F	"Cold Work-Hot Work"	"Hot Work"
800	3	12
950	4	13
1100	5	14
1250	6	15
1400	7	16
1550	8	17
1700	9	18
1850	10	19
2000	11	20

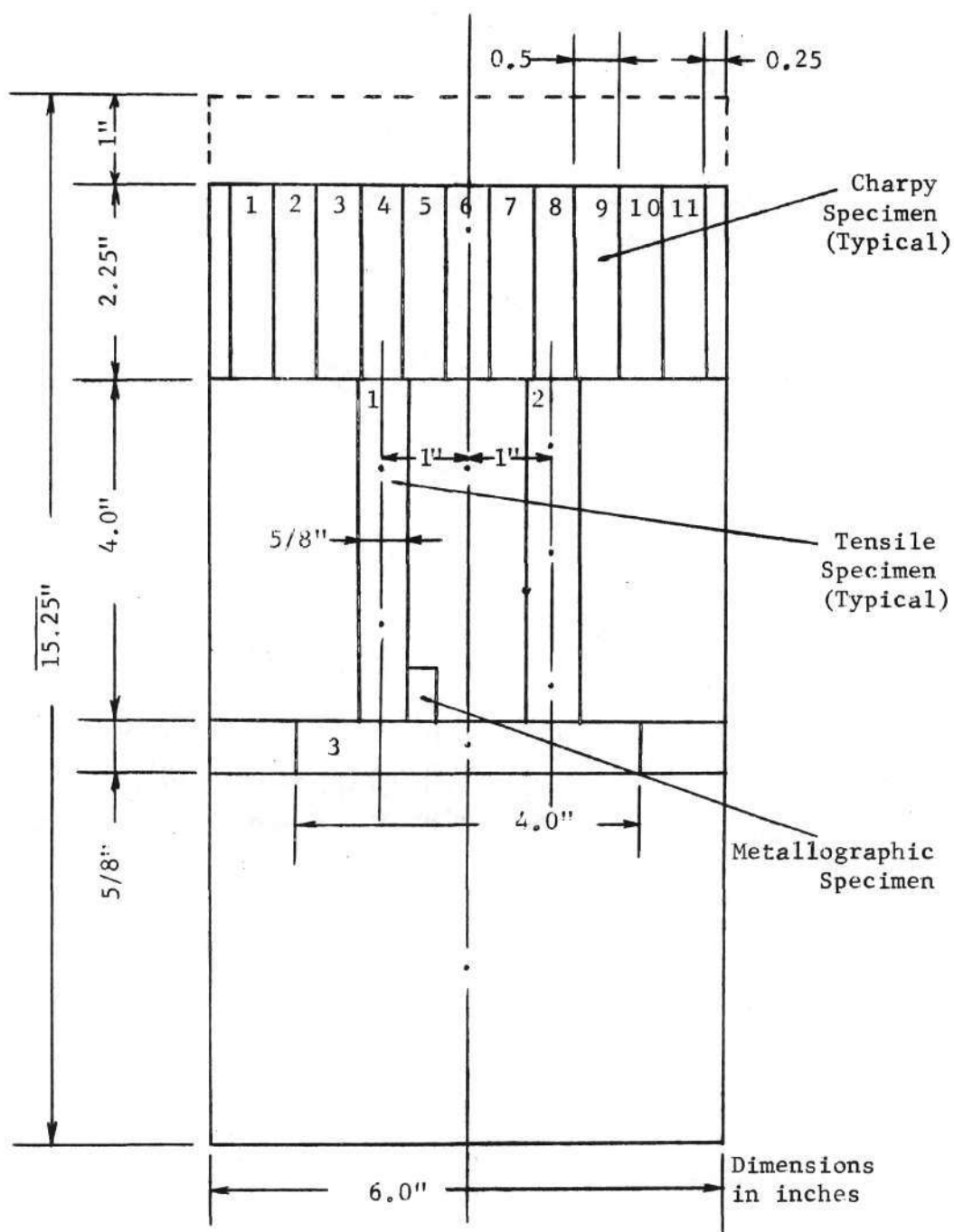


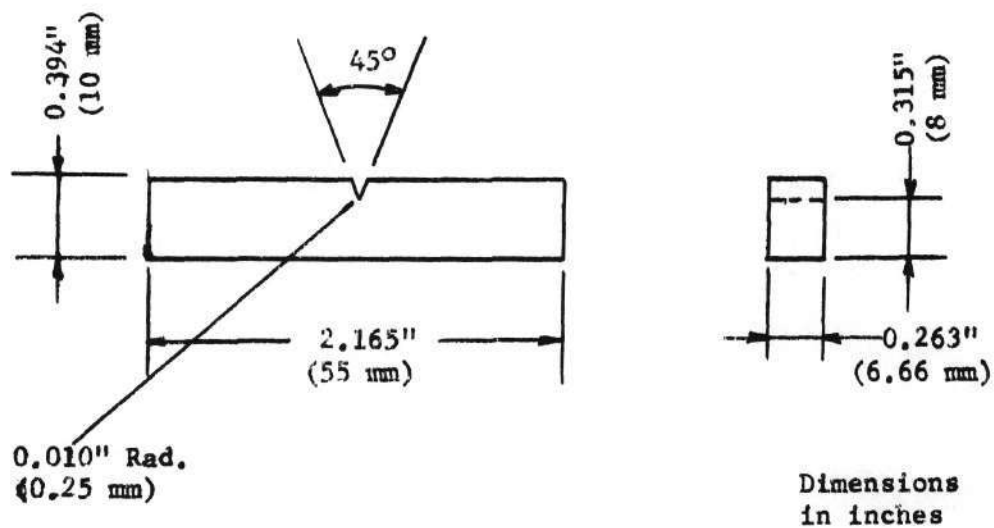
Figure 1. Location of Test Samples Relative to Fabricated Plate

specimens of this "standard" thickness could not be prepared from the sample plates of 0.32 inch fabricated thickness. The two-thirds thickness is a standard compatible with the steel industry practice for sheet and thin plate. The grinding depth was limited to a maximum of 0.005 inch in order to avoid overheating. An adequate supply of cooling water was maintained during grinding to insure that room temperature machining was accomplished. Charpy specimen blanks were then cut from the ground plate sample by use of a DoAll Metalmaster band saw which had a blade of  $1/4$  inch depth and 14 teeth per inch. Each Charpy blank was stamped with the appropriate number in accordance with Table 1. The saw cut surfaces were ground down to the desired width of 10 mm. A standard V-notch of 2 mm depth was machined into each blank by use of a specially prepared cutter mounted on a Milwaukee Model H horizontal milling machine. The dimensions of the Charpy specimens are in accordance with the ASTM Standard E-23. The dimensions are as shown in Figure 2.

#### Tensile Specimens

Two blanks were cut from the sample plate along the longitudinal rolling direction of the plate. One blank was also cut along the transverse direction of the plate. These blanks, which were cut at the location as indicated by Figure 1, were for the eventual preparation of tensile specimens. The blanks were approximately  $5/8$  inch in width. The blanks were then rough turned to approximately 0.30 inch on a Monarch Model 12 CK lathe. Ends were threaded in the same lathe over a length of about one inch ( $1/2$  inch diameter, 13

## Charpy V-Notch Specimen



## Tensile Specimen

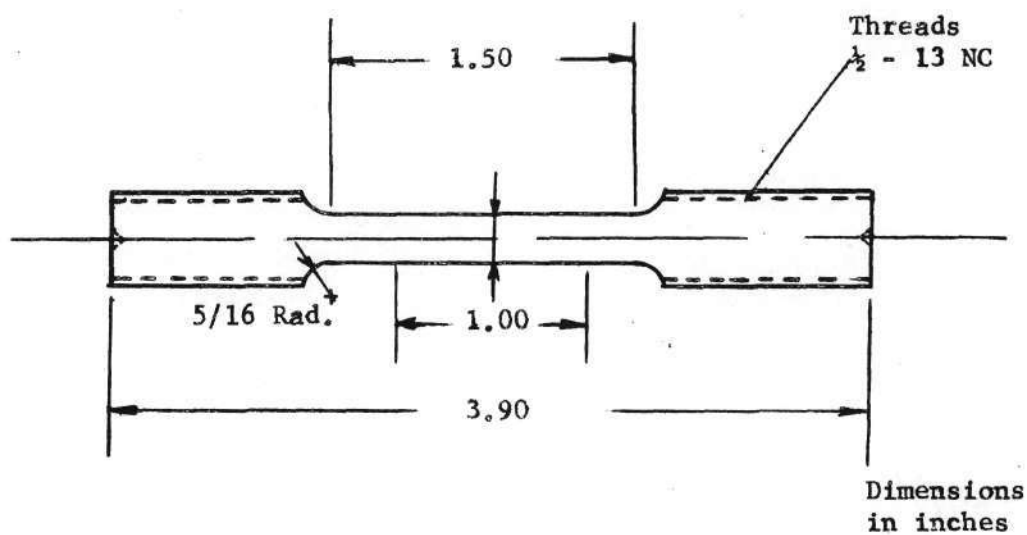


Figure 2. Test Specimen Dimensions

threads per inch). The gage length of each specimen was machined to approximately 0.250 inch diameter in a Monarch Model 14 C lathe equipped with a True Trace Model 106 633 tracer attachment. The final dimensions of the tensile specimens are shown in Figure 2. These dimensions are in accordance with ASTM Standard E-8. The 0.250 inch diameter was necessary because previous experience has shown that at this dimension, tensile specimens will definitely break in the gage length instead of breaking in the threaded ends. These ends have a reduced cross-sectional area resulting from the large flats consistent with the 0.32 inch plate thickness.

#### Metallographic Specimens

Metallographic specimen blanks were cut from each plate sample as indicated in Figure 1. The dimensions of the surface of the blank were 5/8 inch along the longitudinal of the plate and 3/8 inch across the width of the plate. The plate thickness (the cut surface of the blank) was used as the metallographic specimen surface. The blanks were mounted in bakelite. The surface of the specimens were then rough ground in the machine shop while care was taken not to over-heat the surface and thus cause a change in the grain structure. In the next operation, the specimens were ground with AB Carbimet Silicon Carbide papers with grits of 180, 240, 320, 400, and 600. This grinding was done in steps from the 180 wheel to the 600 wheel. The specimens were then polished on an eight inch diameter wheel with a Buehler AB Microcloth. The polishing solution consisted of Buehler Alpha Micropolish, 0.3 micron. A 4 per cent Nital solution was used for etching.

### CHAPTER III

#### EXPERIMENTAL PROCEDURES

##### Tensile Tests

The tensile testing for this investigation was done on the 10,000 pound capacity floor model (Model TTG) Instron machine which belongs to the School of Mechanical Engineering. The tensile specimens were tested at room temperature by the Instron machine which operated at either 10,000 pound or 5,000 pound capacity depending on the steel being elongated. The extensometer which was attached to the test specimens was permitted to indicate elongation readings of either 25 per cent or 50 per cent maximum elongation. The Instron Model G51-12 extensometer was used since it could achieve elongation values which are compatible with tested steel specimens. A crosshead velocity of 0.05 inch per minute was held constant during the testing. Load-elongation diagrams are autographically recorded on 10 inch wide chart paper. The motion of the pen across the 10 inch wide chart paper is actuated by the signal from a load cell, while the X-direction pen travel is proportional to the elongation signal of the extensometer. Maximum size load-elongation diagrams were printed out on the charts by making the proper load capacity and extensometer settings.

Each recorded load-elongation diagram was analyzed to produce such calculated results such as upper yield point and lower

yield point values, or when applicable 0.2 per cent offset yield strength. Yield point elongation was directly measured from those diagrams which showed upper and lower yield points. Uniform elongation to necking and total elongation to fracture were also measured directly from the diagram. The initial specimen diameters were measured by a micrometer from which the initial cross-sectional areas were determined. The cross-sectional area at the fracture was determined by measuring the maximum diameter and the minimum diameter since the fracture area was more elliptical than round. The two measurements were used to figure the elliptical area of the fracture. A Leitz Toolmaker's Model WM II microscope was used to make the two measurements at fracture. The per cent reduction of area values were calculated by comparing the initial areas with the fracture areas. By noting the fracture load, the values of engineering fracture stress and true fracture stress were respectively obtained by dividing the load by the initial cross-sectional area and the fracture cross-sectional area.

Strain hardening effects were analyzed from each recorded load-elongation diagram. For most cases, the value of load on each diagram was noted for each per cent of plastic strain. For those tensile specimens which tended to be brittle and showed little ductility, load values were determined at each half per cent value of strain. These load values were divided by the initial cross-sectional areas to determine the corresponding engineering stresses, and thus engineering stress-strain data for each specimen were compiled

in tabular form. True stress and true strain values, corresponding to the individual engineering stress and strain values, were calculated by application of appropriate formulations. The true stress and true strain values were only calculated from engineering stress and strain values measured before and during the onset of necking.

The strain hardening coefficient  $n$  and the strength coefficient  $K$  were determined by the use of equation (8) with two methods. The first method was by graphical means and the second was by Considère's second finding. In the graphical method,  $\log \bar{\sigma}$  values were plotted against  $\log \bar{\epsilon}$  values, and the  $n$  value was determined from the slope of the line as is indicated by equation (8). These  $n$  values and the maximum load values were used with equation (8) to calculate the  $K$  values. Difficulty resulted when the  $\log \bar{\sigma} - \log \bar{\epsilon}$  plot did not yield a straight line. This was surmounted by evaluating the slope of the last three or four points (maximum loads) which indicated a straight line. In the second method,  $n$  and  $K$  values were obtained by using Considère's second finding which is that the true strain value at necking is equal to  $n$  (when equation (8) is exactly followed). By using these values of  $n$  with maximum load values, the  $K$  values were calculated by using equation (8). In comparing these methods, the two sets of  $n$  and  $K$  values for each test specimen generally showed little deviation except for cases involving severely cold worked materials.

There was an initial total of 60 test specimens. As is nearly always the case with a test program of this scope, some of the specimens necked, deformed and fractured outside the gage length

of the extensometer. For these specimens which were probably undercut at the fillets on the tracer lathe, duplicate specimens were prepared for retesting.

### Charpy Impact Tests

Charpy impact tests were performed on a total of 220 V-notch Charpy specimens which consisted of 11 samples from each of the numerical designated materials of Table 1. A 220 foot-pound capacity Tinius Olsen Charpy-Izod unit was used for the testing.

The objective of the impact testing was the determination of Charpy energy values over the entire transition temperature range from very brittle behavior to very ductile behavior, so as to allow evaluation of the 15 foot-pound transition temperature for each of the designated materials of Table 1. Energy values obtained with the eleven Charpy specimens of each material were plotted against testing temperatures, and the 15 foot-pound transition temperature was directly read from the plot.

During the testing, insulated wide-mouth Thermos flasks were used to confine liquid baths which provided the required variations of test temperatures. Specimens were immersed in the baths for thirty minutes before testing. The bath used for elevated temperature testing was water, and the bath used for temperatures below room temperature was controlled mixtures of ice and water, and table salt. For extreme cold temperatures, baths of dry ice and acetone or liquid nitrogen and ethyl alcohol were used. Once the proper concentrations or mixtures were obtained, baths of remarkable stable temperatures

resulted within one degree Fahrenheit for a relatively long time. Thermometers which could be read to within one-half degree were used in the testing. The maximum elapsed time between the specimen removal from the bath and the rupturing of the test bars by the Charpy machine was five seconds, resulting in little opportunity for a temperature change in the specimen from the stable bath temperature.

#### Hardness Tests

Both Rockwell and Brinell hardness tests were performed on ruptured Charpy specimens since the machined surfaces of these specimens were ideal for such testing. Care was taken to avoid the strain hardened material near the fractured surface of each specimen.

In the Metallography Laboratory of the School of Mechanical Engineering, there is available a Brinell unit manufactured by the Steel City Testing Laboratory of the Tinius Olsen Testing Machine Company. Also available in the same lab is a Rockwell unit made by the Wilson Mechanical Instrument Division, American Chain and Cable Company. Both units were used in the testing.

All Brinell determinations of hardness involved the application of 3,000 kg loads to 10 mm diameter spherical indentors. This combination of load and diameter is the most common for steel specimens.

Approximately ten Rockwell hardness determinations were made for each of the designated materials of Table 1. The B scale was found to be applicable for most of the material, and the usual 1/16 inch diameter ball and 100 kg load were used in the testing. Some materials were harder than the upper limit ( $100 R_B$ ) of the B scale,

and therefore the C scale, with diamond brale and 150 major load, had to be used.

### Metallographic Analysis

Photomicrographs at 400x magnification were prepared from each of the polished and etched metallographic samples. A vertical Vicker's "55" metallograph which belongs to the Metallographic Laboratory of the School of Chemical Engineering was used for the high magnification optical investigations. Polaroid 4 x 5 Land Film, Type 55 P/N was used, and the long dimension of the film was oriented to be in the rolling direction of the plate. This type of Polaroid film produced negatives as well as prints. The negatives were saved for future prints.

Each photomicrograph was prepared to be representative of the entire grain structure of the material. It was noticed that there was little variation in the microstructure throughout the thickness of the fabricated plate samples.

The photomicrographs were used to make quantitative measurements which are associated with mechanical properties. For example, a measured ferrite grain size value could be used in the Hall-Petch relationship, equation (1), to evaluate the yield strength. Grain size and volume fraction of pearlite measurements could be used for equation (4) to evaluate yield strength if the applicable steel in the appropriate condition was considered. The same two quantities could be used to determine the ultimate tensile strength by using equation (8). Other previously discussed relationships (equations (6) and (7)) in

the literature indicate other possible variations of properties with microstructural changes. Cold or warm work would cause a departure from an equiaxed grain structure, resulting in grain elongation in the rolling direction. A quantitative measure of this degree of orientation could be of interest.

The volume fraction of pearlite was determined by the point counting method which required the use of a transparent grid. The grid consisted of sharp dark lines intersecting to make  $1/4$  inch squares. The grid was placed over the photomicrograph such that one set of lines was parallel to the rolling direction and the other set of lines was perpendicular. Depending on the grid size and the size of the photomicrograph, the grid lines will intersect in a number of points on the photomicrograph. The volume fraction of pearlite will be the number of grid intersection points located over the pearlite features divided by the total number of points located in the photomicrograph. The volume fraction of ferrite was determined by the same method. Some of the grid intersection points were located over inclusions such as manganese-sulfide or located over spheroidized cementite.

The grid was also used to establish values of the grain diameter  $d$ . The grain diameter is better referred to as the "mean intercept length" which is the average length of random line intercepted by the average grain. The ferrite mean intercept length using Underwood's (40) symbols is calculated by:

$$d_{\alpha} = \frac{\% \text{ Ferrite}}{100} \times \frac{1}{N_{L\alpha}} \quad (\text{in.}) \quad (11)$$

In this relationship,  $N_{L\alpha}$  is the number of interceptions of ferrite grains per unit of length of grid line ( $\text{inch}^{-1}$ ). Since it is expected to have ferrite-pearlite microstructure, the quantity  $N_{L\alpha}$  is defined as (40):

$$N_{L\alpha} = \frac{2(P_L)_{\alpha\alpha} + (P_L)_{\alpha\beta}}{2} \quad (\text{in}^{-1}) \quad (12)$$

where  $(P_L)_{\alpha\alpha}$  = number of ferrite-ferrite interfaces (grain boundaries) per unit length of grid line

$(P_L)_{\alpha\beta}$  = number of ferrite-pearlite interfaces per unit length of grid line

The following formulations were used to determine  $P_L$ :

$$(P_L)_{\alpha\alpha} = \frac{(P_{\alpha\alpha})_{\parallel} + (P_{\alpha\alpha})_{\perp}}{L_{\parallel} + L_{\perp}} \quad (13)$$

$$(P_L)_{\alpha\beta} = \frac{(P_{\alpha\beta})_{\parallel} + (P_{\alpha\beta})_{\perp}}{L_{\parallel} + L_{\perp}} \quad (14)$$

where  $L_{\parallel}$  = length of the rolling direction grid lines

$L_{\perp}$  = length of the transverse grid lines

$(P_{\alpha\alpha})_{\parallel}$  = total number of intersections of ferrite-ferrite grain boundaries with the rolling direction grid lines

$(P_{\alpha\alpha})_{\perp}$  = total number of intersections of ferrite-ferrite grain boundaries with transverse grid lines

$(P_{\alpha\beta})_{\parallel}$  = total number of intersections of ferrite-pearlite grain boundaries with rolling direction grid lines

$(P_{\alpha\beta})_{\perp}$  = total number of intersections of ferrite-pearlite grain boundaries with transverse grid lines

The pearlite mean intercept length can be evaluated by:

$$d_{\beta} = \frac{(\% \text{ Pearlite})}{100} \times \frac{1}{N_{L\beta}} \quad (\text{in.}) \quad (15)$$

where  $N_{L\beta}$  = number of interceptions of pearlite colonies or patches per unit length of grid line

Since the number of ferrite grains are of no interest, equation (12) becomes:

$$N_{L\beta} = \frac{(P_L)_{\alpha\beta}}{2} \quad (\text{in}^{-1}) \quad (16)$$

The orientation factor  $\alpha$  is an indication of the degree of distortion of ferrite grains. Underwood's defining relationship is:

$$n_{\alpha} = \frac{(N_{L\alpha})_{\perp} - (N_{L\alpha})_{\parallel}}{(N_{L\alpha})_{\perp} + 0.571 (N_{L\alpha})_{\parallel}} \quad (17)$$

where  $(N_{L\alpha})_{\perp}$  = number of interceptions of ferrite grains of the microstructure per unit of length of grid lines normal to the rolling direction

$(N_{L\alpha})_{\parallel}$  = number of interceptions of ferrite grains of the microstructure per unit length of grid lines parallel to the rolling direction

A value of one will be assigned to  $n_{\alpha}$  for a hypothetical perfectly oriented microstructure in which the grains are reduced to lines in the rolling direction. The orientation factor will be zero for grains which are ideally equiaxed. The orientation factor will have values between these limits for a partially oriented structure.

## CHAPTER IV

## RESULTS

Mechanical PropertiesTensile Tests

Tables 2, 3, 4, 5, 6, and 7 summarize all calculated results associated with Instron plotted load-elongation diagrams. The even-numbered tables contain calculated data for "hot-work" tensile specimens, while the odd-numbered tables contain calculated results for the "cold work-hot work" specimens. Yielding properties are considered in Tables 2 and 3 while properties associated with necking are considered in Tables 4 and 5. Fracture properties are summarized in Tables 6 and 7.

Charpy Impact Test

Tables 8 and 9 contain energy values (foot-pounds) resulting from tests on the V-notch Charpy Specimens; Table 8 contains data for the "hot-work" specimens while Table 9 has to do with the "cold work-hot work" material. Charpy energy for each number designated steel was plotted as the ordinate against testing temperature as the abscissa, and values of 15 foot-pound transition temperatures were derived from these plots. Table 10 summarizes these 15 foot-pound transition temperature values.

Hardness Tests

Tables 11 and 12 contain hardness test data. Rockwell B( $R_B$ )

and Rockwell C ( $R_C$ ) test results are included with each value representing the average of six or seven test readings for each of the number designated steels. Brinell test data, which are a result of 3,000 kg loads and 10 mm diameter balls, are also included, and each listed value represents the average of two test readings.

#### Metallographic Analysis

Tables 13 and 14 include quantitative metallographic results obtained from the photomicrographs. The listed values were determined for each photomicrograph. Included are the values for ferrite mean intercept length (grain diameter), volume fraction of pearlite (expressed on a per cent basis), and ferrite orientation factor. Also included in these tables are the calculated values of  $d^{-\frac{1}{2}}$  which is one of the terms used in the Hall-Petch relationship.

Table 2. Tensile Test Results Related  
to Yielding, Hot Work Samples

Code	Finishing Temperature (°F)	Upper Yield Point (psi)	Lower Yield Point (psi)	0.2% Offset Yield Strength (psi)	Yield Point Drop (psi)	Yield Point Elongation %
Longitudinal Specimens						
1L1	mill	62,660	61,070	---	1,590	0.80
1L2	mill	62,960	62,560	---	400	0.90
12L1	800	---	---	129,350	---	---
12L2	800	---	---	132,890	---	---
13L1	950	---	---	106,600	---	---
13L2	950	---	---	107,050	---	---
14L1	1100	92,890	91,870	---	1,020	0.70
14L2	1100	92,560	91,960	---	600	0.55
15L1	1250	81,630	80,580	---	1,050	0.20
15L2	1250	83,890	82,010	---	1,880	0.95
16L1	1400	76,590	71,830	---	4,760	0.80
16L2	1400	78,990	70,640	---	8,350	2.70
17L1	1550	75,540	67,720	---	7,820	2.90
17L2	1550	75,870	68,890	---	6,980	3.60
18L1	1700	69,610	62,940	---	6,670	1.55
18L2	1700	67,040	64,050	---	2,990	2.25
19L1	1850	75,790	67,400	---	8,390	2.00
19L2	1850	62,000	58,370	---	3,630	0.90
20L1	2000	---	---	60,030	---	---
20L2	2000	58,430	57,600	---	830	0.20
Transverse Specimens						
1T	mill	65,360	62,750	---	2,610	0.80
12T	800	---	---	128,340	---	---
13T	950	---	---	108,330	---	---
14T	1100	---	---	94,180	---	---
15T	1250	85,140	84,310	---	830	0.30
16T	1400	79,160	69,820	---	9,340	2.25
17T	1550	75,140	69,240	---	5,900	3.10
18T	1700	68,510	62,250	---	6,260	1.30
19T	1850	67,640	63,860	---	3,780	1.60
20T	2000	---	---	62,070	---	---

Table 3. Tensile Test Results Related to  
Yielding, Cold Work-Hot Work Samples

Finishing Code Temperature (°F)	Upper Yield Point (psi)	Lower Yield Point (psi)	0.2% Offset Yield Strength (psi)	Yield Point Drop (psi)	Yield Point Elongation %
Longitudinal Specimens					
2L1 Cold Rolled	---	---	104,250	---	---
2L2 Cold Rolled	---	---	106,570	---	---
3L1 800	---	---	127,310	---	---
3L2 800	---	---	128,340	---	---
4L1 950	---	---	111,400	---	---
4L2 950	---	---	110,270	---	---
5L1 1100	---	---	94,800	---	---
5L2 1100	---	---	95,290	---	---
6L1 1250	---	---	82,800	---	---
6L2 1250	---	---	74,860	---	---
7L1 1400	74,930	69,340	---	5,590	2.25
7L2 1400	74,480	67,960	---	6,520	2.10
8L1 1550	66,610	62,130	---	4,480	2.10
8L2 1550	70,380	66,550	---	3,830	1.45
9L1 1700	66,270	58,910	---	7,360	1.60
9L2 1700	62,600	57,070	---	5,530	1.20
10L1 1850	62,070	55,330	---	6,740	1.00
10L2 1850	56,840	54,270	---	2,570	1.30
11L1 2000	---	---	55,950	---	---
11L2 2000	56,890	55,980	---	910	0.45
Transverse Specimens					
2T Cold Rolled	---	---	100,260	---	---
3T 800	---	---	127,310	---	---
4T 950	---	---	111,620	---	---
5T 1100	---	---	96,780	---	---
6T 1250	80,600	76,800	---	3,800	1.60
7T 1400	60,110	58,840	---	1,270	1.50
8T 1550	69,300	64,070	---	5,230	1.20
9T 1700	65,640	60,590	---	5,050	2.30
10T 1850	60,750	57,740	---	3,010	1.10
11T 2000	---	---	56,490	---	---

Table 4. Tensile Test Results Related  
to Necking, Hot Work Samples

Code	Finishing	Ultimate Tensile Strength	Uniform Elongation	Strain Hardening		Strength	
	Temperature			Exponent n	Coefficient K		
	(°F)						UTS
Longitudinal Specimens							
1L1	mill	90,310	14.3	0.1337	0.1293	135,090	133,890
1L2	mill	90,590	13.7	0.1284	0.1336	134,050	135,470
12L1	800	136,080	4.1	0.0402	0.0505	161,190	166,400
12L2	800	138,450	4.0	0.0392	0.0429	163,490	165,400
13L1	950	121,710	6.5	0.0630	0.0729	154,280	158,440
13L2	950	120,620	5.4	0.0526	0.0638	148,430	153,220
14L1	1100	107,350	8.3	0.0797	0.0851	142,240	144,170
14L2	1100	107,720	8.6	0.0825	0.0843	143,720	144,360
15L1	1250	96,990	9.5	0.0908	0.0968	132,050	133,950
15L2	1250	98,080	10.0	0.0953	0.0994	134,980	136,270
16L1	1400	91,600	11.7	0.1106	0.1219	130,530	133,730
16L2	1400	90,150	12.7	0.1196	0.1200	130,970	131,090
17L1	1550	87,750	17.5	0.1613	0.1600	138,380	138,060
17L2	1550	87,370	18.2	0.1672	0.1658	139,270	138,930
18L1	1700	85,010	14.5	0.1354	0.1350	127,600	127,500
18L2	1700	86,530	15.3	0.1424	0.1486	131,684	133,270
19L1	1850	87,110	14.9	0.1389	0.1379	131,660	131,390
19L2	1850	84,350	15.8	0.1467	0.1508	129,450	130,470
20L1	2000	89,200	13.8	0.1293	0.1264	132,240	131,470
20L2	2000	87,860	15.1	0.1406	0.1392	133,240	132,880
Transverse Specimens							
1T	mill	91,920	13.6	0.1275	0.1308	135,780	136,710
12T	800	139,950	3.7	0.0363	0.0375	163,700	164,330
13T	950	121,870	5.7	0.0554	0.0625	151,220	154,270
14T	1100	109,290	6.6	0.0639	0.0610	138,900	137,790
15T	1250	98,710	7.6	0.0733	0.0705	128,620	127,690
16T	1400	88,600	14.1	0.1319	0.1342	132,060	132,670
17T	1550	89,110	16.9	0.1562	0.1564	139,210	139,290
18T	1700	86,400	16.0	0.1484	0.1625	133,020	136,560
19T	1850	87,730	11.8	0.1115	0.1214	125,260	127,950
20T	2000	91,000	10.5	0.0998	0.0977	126,560	125,940

Table 5. Tensile Test Results Related to Necking, Cold Work-Hot Work Samples

Code	Finishing Temperature (°F)	Ultimate Tensile Strength (psi)	Uniform Elongation %	Strain Hardening		Strength Coefficient K	
				UTS	Exponent n Graph.	UTS (psi)	Graph. (psi)
Longitudinal Specimens							
2L1	Cold Rolled	111,870	1.2	0.0119	0.0114	119,350	119,060
2L2	Cold Rolled	112,690	1.3	0.0129	0.0125	120,750	120,530
3L1	800	134,320	3.8	0.0373	0.0333	157,620	155,500
3L2	800	136,830	4.2	0.0411	0.0500	162,570	167,080
4L1	950	121,740	5.8	0.0564	0.0631	151,480	154,380
4L2	950	120,490	5.5	0.0535	0.0478	148,690	146,140
5L1	1100	107,850	7.3	0.0705	0.0767	139,500	141,800
5L2	1100	109,010	7.6	0.0733	0.0783	142,050	143,910
6L1	1250	92,110	9.1	0.0871	0.0852	124,300	123,710
6L2	1250	90,450	10.1	0.0962	0.0970	124,740	124,970
7L1	1400	90,660	14.4	0.1345	0.1338	135,850	135,610
7L2	1400	91,310	13.1	0.1231	0.1238	133,650	133,830
8L1	1550	85,250	17.0	0.1570	0.1520	133,390	132,150
8L2	1550	87,350	15.1	0.1406	0.1463	132,480	133,960
9L1	1700	83,740	16.5	0.1527	0.1536	129,980	130,190
9L2	1700	83,470	14.7	0.1372	0.1329	125,730	124,650
10L1	1850	83,110	15.6	0.1450	0.1392	127,110	125,680
10L2	1850	82,590	15.9	0.1476	0.1475	126,960	126,940
11L1	2000	87,330	13.4	0.1258	0.1319	128,530	130,160
11L2	2000	86,700	12.5	0.1178	0.1206	125,480	126,250
Transverse Specimens							
2T	Cold Rolled	112,490	2.6	0.0257	0.0225	126,790	125,310
3T	800	138,060	3.7	0.0363	0.0475	161,490	167,320
4T	950	123,330	5.0	0.0488	0.0556	150,060	153,120
5T	1100	109,620	6.5	0.0630	0.0660	138,950	140,100
6T	1250	91,070	9.2	0.0880	0.1034	123,160	127,690
7T	1400	84,390	15.8	0.1467	0.1476	129,510	129,730
8T	1550	85,420	16.5	0.1527	0.1540	132,600	132,910
9T	1700	84,160	17.2	0.1587	0.1583	132,100	132,000
10T	1850	85,410	12.1	0.1142	0.1181	122,660	123,700
11T	2000	87,330	12.2	0.1151	0.1194	125,680	126,830

Table 6. Tensile Test Results Related to Fracture, Hot Work Samples

Code	Finishing Temperature (°F)	Engineering Fracture Stress (psi)	True Fracture Stress (psi)	Reduction of Area %	Elongation %
------	-------------------------------	--------------------------------------	-------------------------------	------------------------	-----------------

Longitudinal Specimens

1L1	mill	67,440	168,740	60.0	26.0
1L2	mill	68,090	175,130	61.1	25.0
12L1	800	102,880	188,430	45.4	12.2
12L2	800	107,420	193,900	44.6	11.6
13L1	950	93,360	181,930	48.7	15.9
13L2	950	93,490	180,570	48.2	13.7
14L1	1100	79,040	181,990	56.6	19.3
14L2	1100	80,440	179,040	55.1	19.3
15L1	1250	70,170	175,070	59.9	21.5
15L2	1250	73,040	159,530	54.2	22.1
16L1	1400	64,170	186,300	65.6	23.9
16L2	1400	64,590	184,560	65.0	25.7
17L1	1550	60,310	184,780	67.4	31.4
17L2	1550	61,400	177,030	65.3	33.0
18L1	1700	59,750	177,660	66.4	21.3
18L2	1700	59,480	190,810	68.8	30.0
19L1	1850	70,940	168,510	57.9	24.6
19L2	1850	59,820	180,180	66.8	30.0
20L1	2000	64,380	184,270	65.1	30.1
20L2	2000	62,400	168,740	63.0	30.4

Transverse Specimens

1T	mill	74,180	163,070	54.5	25.0
12T	800	121,210	170,290	28.8	7.6
13T	950	104,690	160,420	34.7	11.3
14T	1100	92,940	156,280	40.5	13.3
15T	1250	82,430	153,520	46.3	16.7
16T	1400	71,050	164,530	56.8	24.4
17T	1550	71,410	166,510	57.1	29.4
18T	1700	69,730	161,590	56.9	28.5
19T	1850	68,630	169,620	59.5	22.9
20T	2000	72,270	169,800	57.4	21.1

Table 7. Tensile Test Results Related to Fracture, Cold Work-Hot Work Samples

Code	Finishing Temperature (°F)	Engineering Fracture Stress (psi)	True Fracture Stress (psi)	Reduction of Area (%)	Elongation (%)
Longitudinal Specimens					
2L1	Coiled Rolled	82,400	180,180	54.3	11.8
2L2	Coiled Rolled	82,500	190,870	56.8	12.1
3L1	800	102,450	191,030	46.4	11.5
3L2	800	104,530	190,490	45.1	12.8
4L1	950	93,300	180,730	48.4	14.9
4L2	950	93,240	215,280	56.7	14.5
5L1	1100	80,520	171,140	52.9	18.1
5L2	1100	81,960	180,460	54.6	17.7
6L1	1250	62,100	174,930	64.5	25.0
6L2	1250	67,630	199,640	66.1	24.2
7L1	1400	64,170	181,820	64.7	28.2
7L2	1400	62,910	179,690	65.0	25.8
8L1	1550	59,280	169,190	65.0	33.1
8L2	1550	61,480	185,510	66.9	28.4
9L1	1700	58,490	170,130	65.6	30.7
9L2	1700	59,470	182,690	67.4	28.7
10L1	1850	58,070	169,530	65.7	29.9
10L2	1850	58,420	173,400	66.3	30.9
11L1	2000	64,140	172,320	62.8	26.3
11L2	2000	62,650	179,090	65.0	26.0
Transverse Specimens					
2T	Coiled Rolled	88,420	163,150	45.8	11.2
3T	800	117,760	166,290	29.2	8.0
4T	950	105,430	179,660	41.3	10.5
5T	1100	92,150	159,850	42.4	13.3
6T	1250	70,330	153,450	54.2	20.8
7T	1400	59,330	171,870	65.5	30.5
8T	1550	68,480	159,950	57.2	28.3
9T	1700	65,220	155,310	58.0	29.3
10T	1850	67,160	164,540	59.2	22.7
11T	2000	68,630	161,600	57.5	24.0

Table 8. Charpy Test Results,  
Hot Work Samples

Code	Temperature (°F)	Energy (Ft-lb.)	Code	Temperature (°F)	Energy (Ft-lb.)
1	- 87	2.0	12	-105	1.0
1	- 65	2.5	12	- 50	1.0
1	- 40	5.0	12	- 25	1.0
1	- 20	12.0	12	+ 34	1.0
1	+ 5	14.0	12	+ 40	2.0
1	+ 12	18.0	12	+ 55	6.0
1	+ 32	27.0	12	+ 60	4.0
1	+ 55	23.0	12	+ 80	3.0
1	+ 72	23.0	12	+100	8.0
1	+ 80	28.0	12	+120	6.0
1	+212	30.0	12	+140	23.0
			12	+208	19.0
13	-105	1.0	14	- 85	2.0
13	- 50	2.0	14	- 58	3.0
13	- 25	1.0	14	- 40	2.0
13	0	8.0	14	- 13	4.0
13	+ 10	4.0	14	- 13	6.0
13	+ 15	17.0	14	+ 12	11.0
13	+ 20	8.0	14	+ 14	10.0
13	+ 34	6.0	14	+ 20	7.0
13	+ 40	15.0	14	+ 33	28.0
13	+ 80	15.0	14	+ 55	34.0
13	+140	23.0	14	+ 77	27.0
13	+208	24.0	14	+212	34.0
15	- 78	4.0	16	-105	1.0
15	- 65	5.0	16	- 90	3.0
15	- 40	5.0	16	- 75	5.0
15	- 20	7.0	16	- 60	4.0
15	+ 5	30.0	16	- 50	17.0
15	+ 12	18.0	16	- 40	22.0
15	+ 20	18.0	16	- 25	10.0
15	+ 32	31.0	16	+ 12	40.0
15	+ 40	30.0	16	+ 34	41.0
15	+ 55	40.0	16	+ 55	44.0
15	+ 73	32.0	16	+ 80	48.0
15	+200	42.0	16	+208	46.0

Table 8. Charpy Tests Results, Hot Work Samples  
(Continued)

Code	Temperature (°F)	Energy (Ft-lb.)	Code	Temperature (°F)	Energy (Ft-lb.)
17	-105	22.0	18	-105	14.0
17	-105	22.0	18	-105	18.0
17	-90	36.0	18	-90	31.0
17	-75	24.0	18	-75	27.0
17	-50	45.0	18	-50	38.0
17	-25	45.0	18	-25	33.0
17	+33	53.0	18	+12	50.0
17	+79	53.0	18	+34	55.0
17	+192	52.0	18	+80	54.0
			18	+208	55.0
19	-85	2.0	20	-105	2.0
19	-60	2.0	20	-105	2.0
19	-35	4.0	20	-75	5.0
19	0	2.5	20	-50	2.0
19	0	3.5	20	-25	4.0
19	+32	3.5	20	-12	4.0
19	+40	57.0	20	0	20.0
19	+55	62.0	20	+12	34.0
19	+70	16.2	20	+34	26.0
19	+140	61.0	20	+80	38.0
19	+209	20.2	20	+140	48.0

Table 9. Charpy Test Results,  
Cold Work-Hot Work Samples

Code	Temperature (°F)	Energy (Ft-lb.)	Code	Temperature (°F)	Energy (Ft-lb.)
2	-110	1.0	3	-94	2.0
2	-50	2.0	3	-58	2.0
2	-25	3.0	3	-36	2.5
2	-10	3.0	3	-4	3.0
2	0	3.0	3	0	5.0
2	+15	3.0	3	+33	3.0
2	+32	25.0	3	+40	2.0
2	+40	4.0	3	+55	2.0
2	+55	7.0	3	+76	3.0
2	+85	29.0	3	+76	8.5
2	+140	30.0	3	+140	12.0
2	+208	38.0	3	+203	17.0
4	-85	2.0	5	-89	2.0
4	-60	2.0	5	-65	2.5
4	-35	4.0	5	-40	5.0
4	0	2.5	5	-20	12.0
4	0	3.5	5	+5	14.0
4	+32	4.5	5	+12	8.0
4	+40	7.0	5	+20	21.0
4	+55	13.0	5	+32	27.0
4	+76	16.0	5	+55	18.0
4	+100	24.0	5	+72	23.0
4	+140	31.0			
4	+209	20.2			
6	-105	1.0	7	-105	2.0
6	-50	1.0	7	-105	26.0
6	-25	2.0	7	-90	27.0
6	-12	3.0	7	-75	11.0
6	-6	5.0	7	-60	28.0
6	0	26.0	7	-50	25.0
6	+12	22.0	7	-25	34.0
6	+34	27.0	7	+34	48.0
6	+55	31.0	7	+80	48.0
6	+80	37.0			
6	+140	48.0			
6	+208	41.0			

Table 9. Charpy Test Results,  
Cold Work-Hot Work Samples  
(Continued)

Code	Temperature (°F)	Energy (Ft-lb.)	Code	Temperature (°F)	Energy (Ft-lb.)
8	-105	8.0	9	-105	12.0
8	-105	25.0	9	-105	23.0
8	-90	36.0	9	-90	25.0
8	-75	32.0	9	-75	21.0
8	-50	39.0	9	-50	24.0
8	-25	43.0	9	-25	36.0
8	+34	46.0	9	+12	55.0
8	+80	54.0	9	+34	44.0
8	+208	52.0	9	+80	60.0
			9	+208	52.0
10	-105	3.0	11	-105	1.0
10	-105	4.0	11	-60	4.0
10	-90	25.0	11	-50	4.0
10	-75	17.0	11	-40	5.0
10	-50	19.0	11	-25	6.0
10	-25	21.0	11	-6	16.0
10	+12	41.0	11	+12	13.0
10	+34	54.0	11	+34	24.0
10	+80	54.0	11	+55	37.0
10	+208	51.0	11	+80	40.0
			11	+208	53.0

Table 10. V-Notch Charpy Transition Temperature

Hot Work		Cold Work-Hot Work	
Code	15 Ft-lb. Transition (°F)	Code	15 Ft-lb. Transition (°F)
1	+ 9	2	+ 67
12	+129	3	+178
13	+ 78	4	+ 67
14	+ 30	5	+ 17
15	+ 8	6	+ 6
16	- 52	7	- 99
17	-122	8	-117
18	-108	9	-103
19	+ 34	10	- 73
20	+ 6	11	+ 13

Table 11. Hardness Test Results,  
Hot Work Samples

Code	Finishing Temperature (°F)	Rockwell B	Rockwell C	Brinnell 3000 Kg. 10 mm Ball
1	Mill	83	---	159
12	800	---	27	223
13	950	---	24	217
14	1100	94	---	192
15	1250	90	---	183
16	1400	90	---	156
17	1550	84	---	137
18	1700	81	---	134
19	1850	84	---	146
20	2000	84	---	143

Table 12. Hardness Test Results,  
Cold Work-Hot Work Samples

Code	Finishing Temperature (°F)	Rockwell B	Rockwell C	Brinnell 3000 Kg. 10 mm Ball
2	Cold Rolled	97	---	201
3	800	---	27	217
4	950	---	24	241
5	1100	96	---	197
6	1250	93	---	170
7	1400	79	---	143
8	1550	82	---	140
9	1700	84	---	146
10	1850	78	---	137
11	2000	83	---	146

Table 13. Optical Metallographic Results,  
Hot Work Samples

Code	Finishing Temperature (°F)	Magnification	Ferrite Mean Intercept (d) (in $\times 10^{-4}$ )	$d^{-1/2}$ in $^{-1/2}$	Pearlite %	Ferrite Orientation Factor %
1	Mill	400x	5.93	41.1	45	8.3
12	800	400x	3.94	50.4	50	47.1
13	950	400x	4.29	48.3	45	56.0
14	1100	400x	4.10	49.4	56	53.5
15	1250	400x	3.94	50.4	52	56.8
16	1400	400x	2.83	59.4	45	45.1
17	1550	400x	2.82	59.6	36	14.8
18	1700	400x	4.40	47.7	42	29.3
19	1850	400x	3.82	51.2	43	9.3
20	2000	400x	3.95	50.3	49	19.0

Table 14. Optical Metallographic Results,  
Cold Work-Hot Work Samples

Code	Finishing Temperature (°F)	Magnification	Ferrite Mean Intercept (d) (in $\times 10^{-4}$ )	$d^{-1/2}$ in $^{-1/2}$	Pearlite %	Ferrite Orientation Factor %
2	Cold Rolled	400x	5.17	44.0	46	50.3
3	800	400x	4.43	47.5	53	47.7
4	950	400x	4.03	49.8	50	53.1
5	1100	400x	4.75	45.9	35	62.2
6	1250	400x	5.42	43.0	36	51.4
7	1400	400x	2.62	61.7	50	13.9
8	1550	400x	2.70	60.8	20	15.3
9	1700	400x	4.02	49.9	31	8.0
10	1850	400x	4.03	49.8	45	22.4
11	2000	400x	3.46	53.7	55	10.6

## CHAPTER V

### DISCUSSION

#### General

The calculated values of the mechanical properties and the metallographic quantitative results of both the "hot-work" material and the "cold work-hot work" material are evaluated against the fabrication temperatures in this section of the text. The mechanical properties of the cold work-hot work material are compared to the mechanical properties of the hot work material. Mechanical properties which were a result of 1400°F to 1700°F fabrication are compared to the mechanical properties of the material in the mill condition. Photomicrographs of the hot work material are shown in this chapter of the text also.

#### Lower Yield Strength

The lower yield strength of the hot work material is plotted against the fabrication temperature in Figure 3. The lower yield strength of the cold work-hot work material is also shown in Figure 4.

#### Hot Work Material

Data are shown in Figure 3 for both the longitudinal and transverse tensile specimens. The longitudinal and transverse data seem to have approximately the same stress values at each fabrication temperature. In a temperature range of 800°F to 1400°F, the yield strength values are comparatively high, and work hardening effects

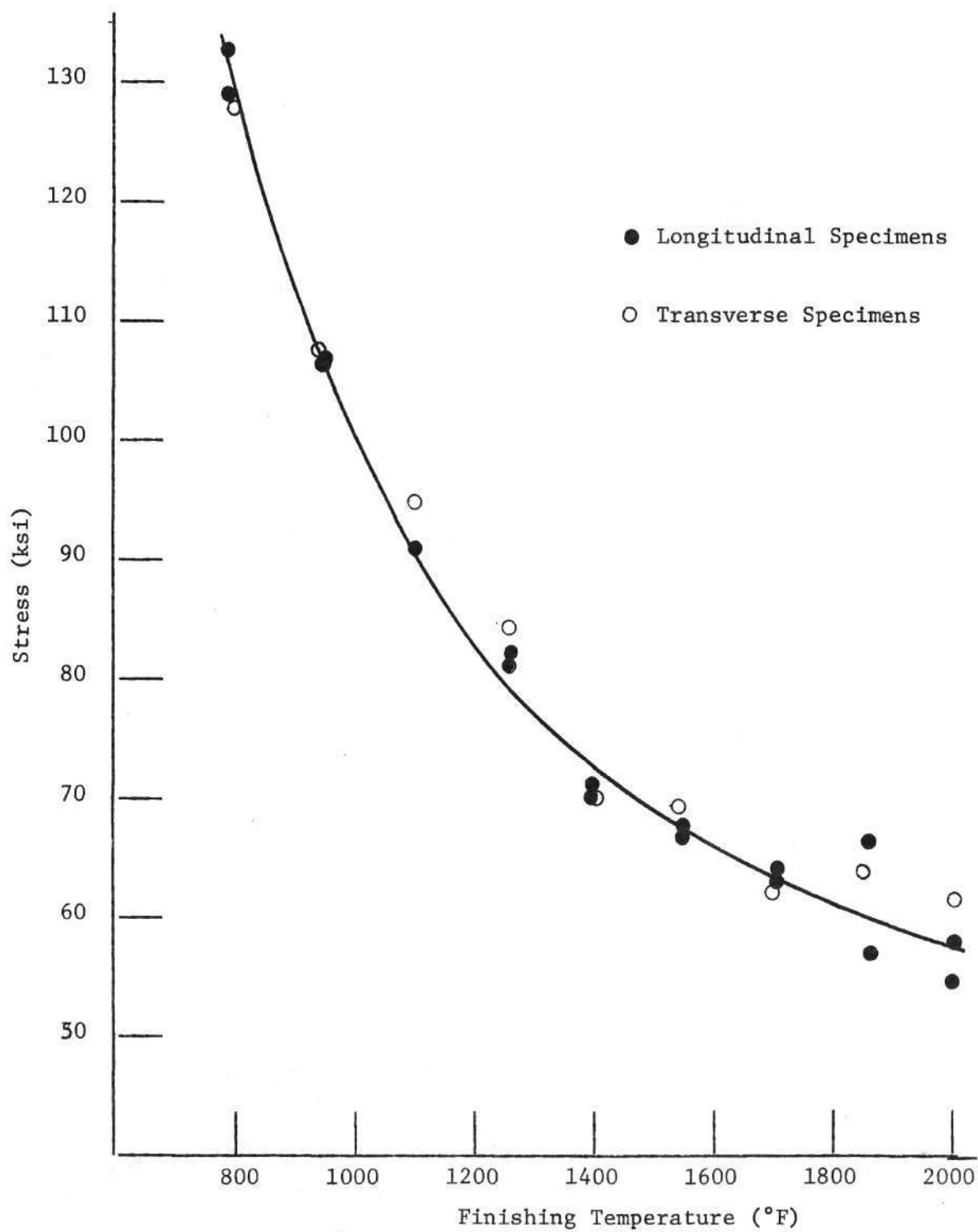


Figure 3. Lower Yield Strength as a Function of Fabrication Temperature, Hot Work Specimens.

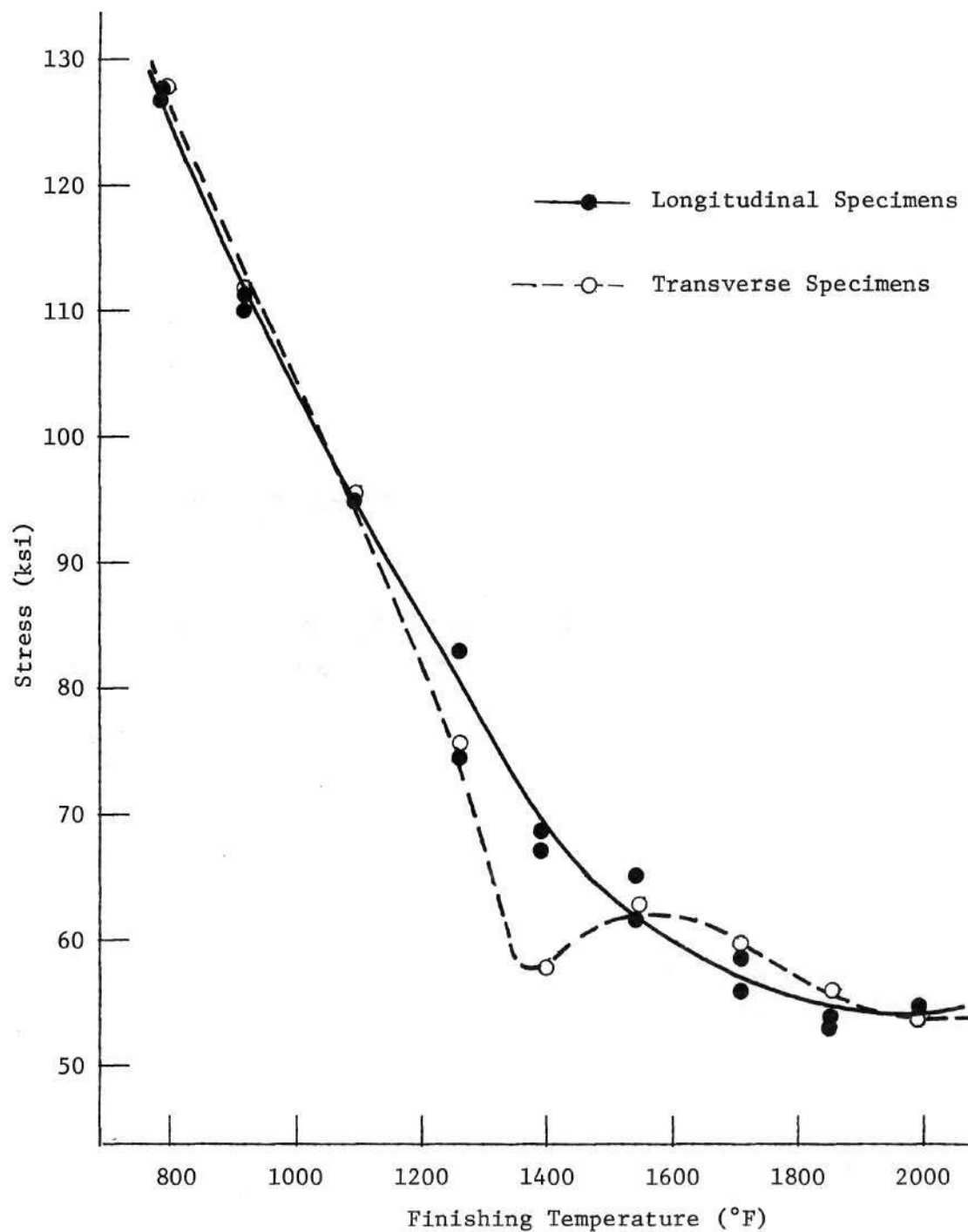


Figure 4. Lower Yield Strength as a Function of Fabrication Temperature, Cold Work-Hot Work Specimens.

apply in this fabrication range. From  $1400^{\circ}\text{F}$  to  $2000^{\circ}\text{F}$ , the yield strength values are comparatively low, and it appears that the yield strength is influenced by the change in grain diameter. The change of grain diameter with fabrication temperature is discussed in more detail in the section on the ferrite mean intercept diameter.

#### Cold Work-Hot Work Material

Figure 4 shows that the behavior of the cold work-hot work material lower yield strength does not differ too significantly from the lower yield strength behavior of the hot work material (Figure 3) with the possible exception of the cold work-hot work transverse specimens. The yield point values of these transverse items in a fabrication temperature range of  $1250^{\circ}\text{F}$  to  $1400^{\circ}\text{F}$  differ significantly from the yield point values of the longitudinal specimens. This can be explained from the anisotropy in the longitudinal direction. In a fabrication temperature range of  $800^{\circ}\text{F}$  to  $1300^{\circ}\text{F}$ , the lower yield strength has approximately the same values as those of the hot work specimens, and preliminary cold working gives no increase in strength. From  $1400^{\circ}\text{F}$  to  $2000^{\circ}\text{F}$ , the yield strength is lower than the yield strength of the hot work material. Although the grain sizes are smaller (see discussion on ferrite mean intercept diameter), this phenomenon can be explained from the fact that the cold work-hot work microstructure does not have as many precipitation hardening particles as the hot work microstructure due to the slower rate of recrystallization of the cold work-hot work material.

### Ultimate Tensile Strength

The ultimate tensile strength of the hot work material is plotted against the fabrication temperature in Figure 5. The ultimate tensile strength of the cold work-hot work material is also shown in Figure 6.

#### Hot Work Material

It appears in Figure 5 that the ultimate tensile strength values of both the longitudinal and the transverse specimens are the same. In a temperature range of 800°F to 1400°F, the ultimate tensile strength values are comparatively high, and work hardening effects apply in this fabrication range. From 1400°F to 2000°F, the tensile strength values are comparatively low. The work hardening effects seem to lose their influence at a temperature of 1400°F which probably corresponds to the eutectoid temperature.

#### Cold Work-Hot Work Material

Figure 6 shows that the ultimate tensile strength values are approximately the same for both the longitudinal specimens and the transverse specimens. Figure 6 also indicates that the ultimate tensile strength behavior does not differ much from the ultimate tensile strength behavior of the hot work material (Figure 5), and thus it is concluded that preliminary cold working has little effect on the ultimate tensile strength.

### Hall-Petch Equation

The applicability of the Hall-Petch equation to the hot work material is considered in Figure 7. The applicability of the equation

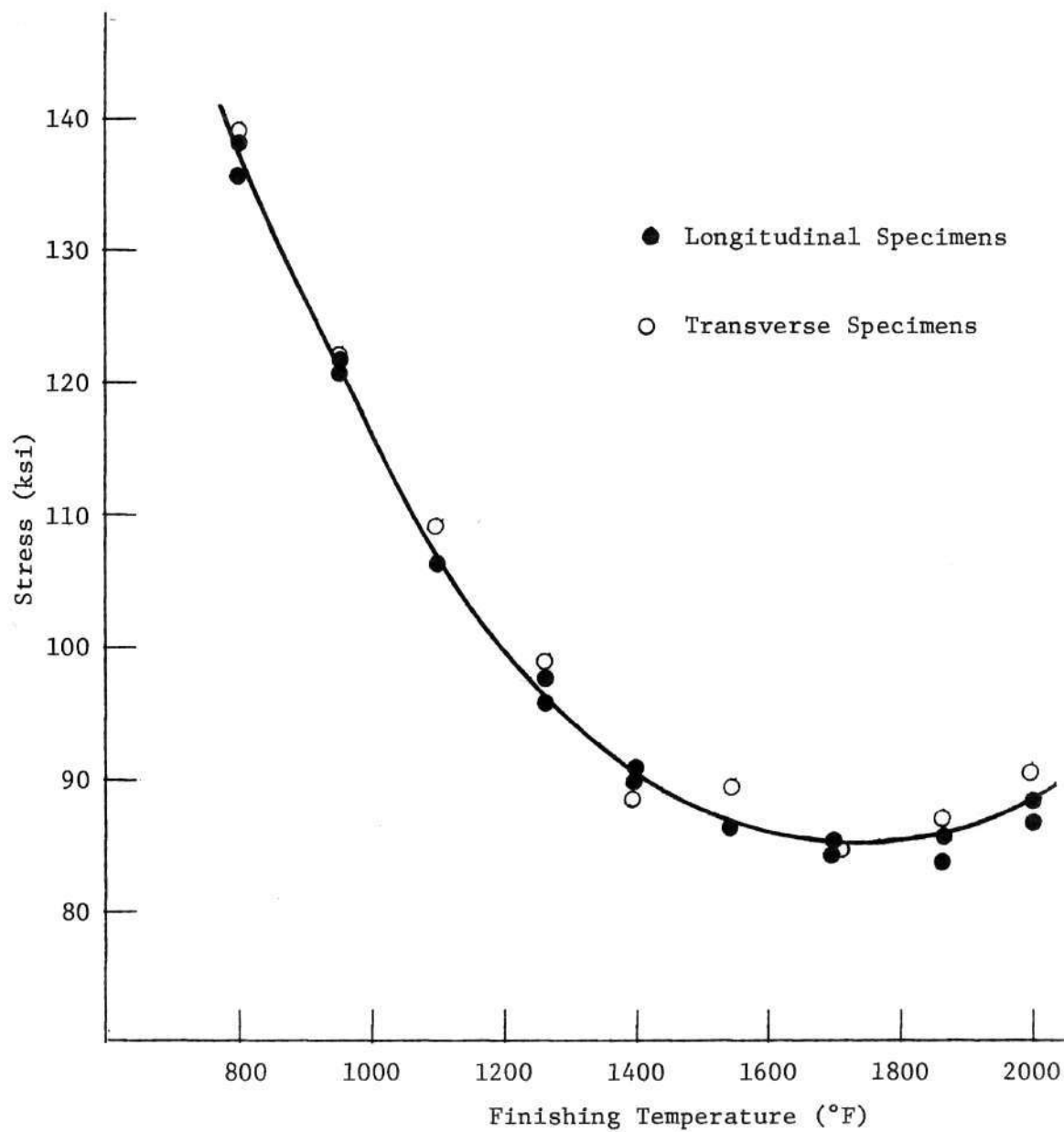


Figure 5. Ultimate Tensile Strength as a Function of  
Fabrication Temperature, Hot Work Specimens.

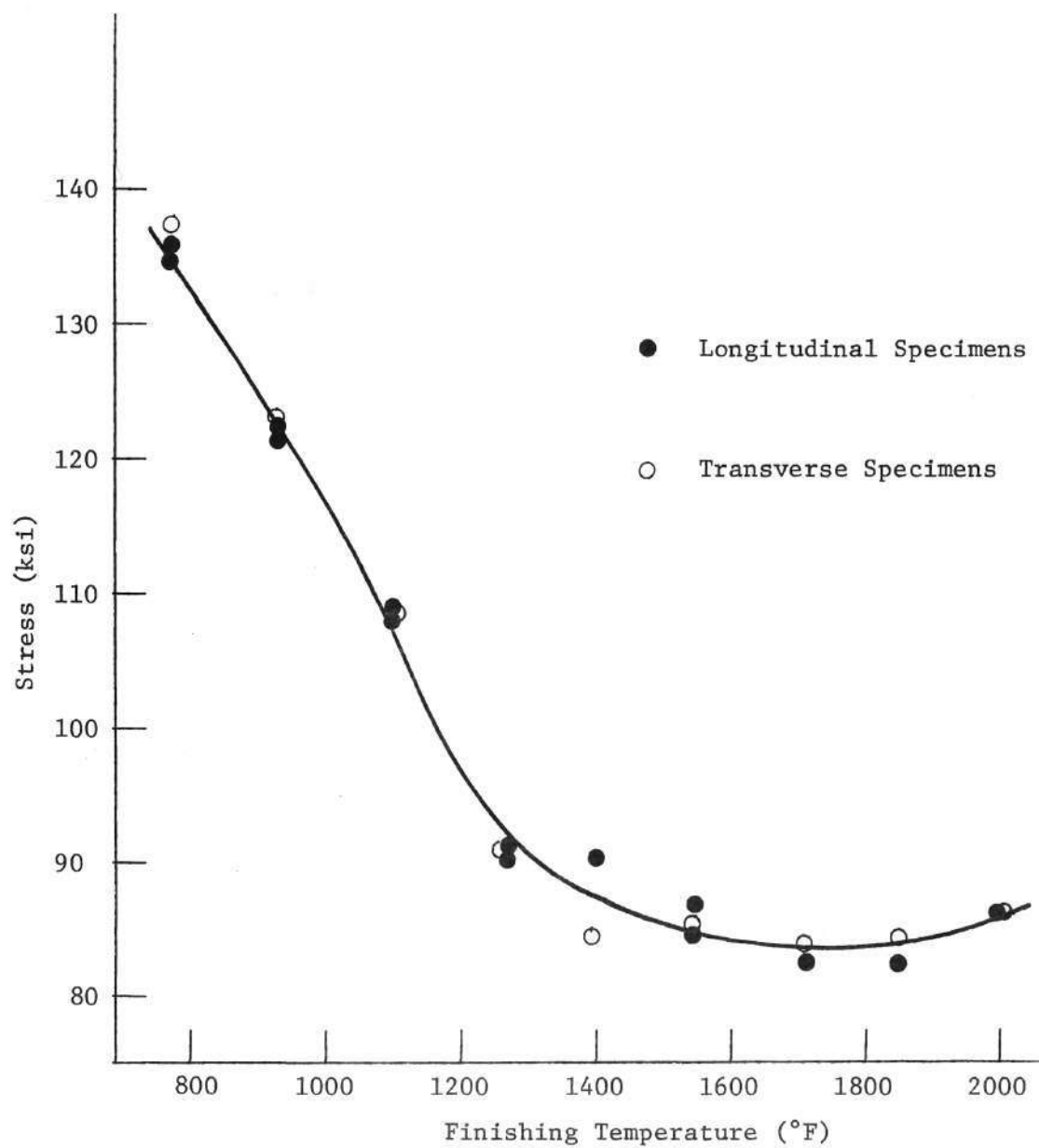


Figure 6. Ultimate Tensile Strength as a Function of Fabrication Temperature, Cold Work-Hot Work Specimens.

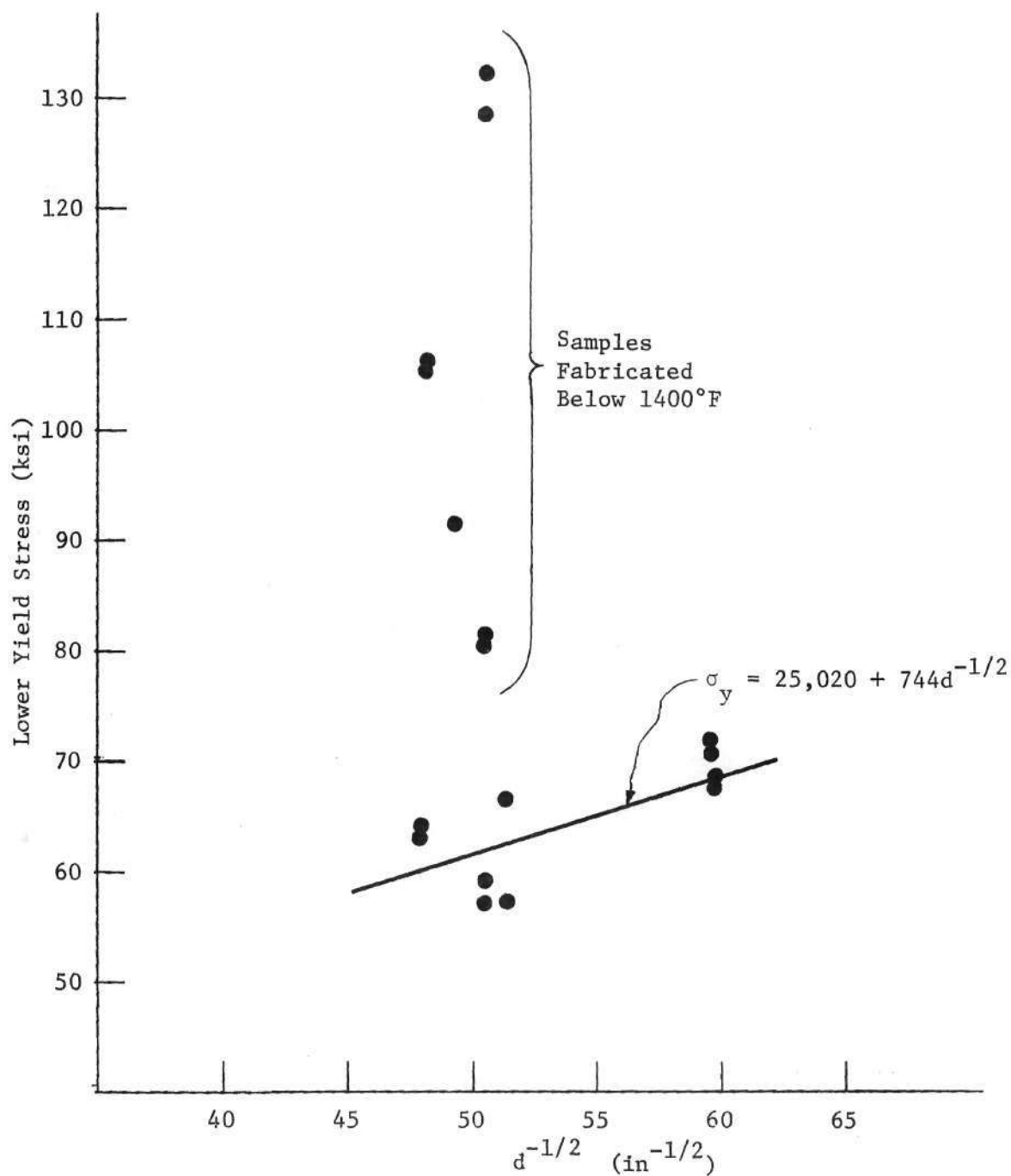


Figure 7. Applicability of the Hall-Petch Equation, Hot Work Longitudinal Specimens.

to the cold work-hot work material is also considered in Figure 8.

#### Hot Work Material

The lower yield strength was plotted against the ferrite grain diameter parameter  $d^{-\frac{1}{2}}$  in Figure 7. For materials fabricated below 1400°F, the yield stress varies, but there is no correlation with grain diameter. This is not surprising since this material is undergoing recovery, and there is no appreciable grain growth. For material fabricated at 1400°F and above, linear regression analysis formulated a Hall-Petch relationship as shown in the figure. The correlation coefficient of 0.7566 indicates that there is a reasonable correlation between the lower yield strength and  $d^{-\frac{1}{2}}$ .

#### Cold Work-Hot Work Material

The same conclusions that were discussed for Figure 7 can be applied to Figure 8. The correlation coefficient of 0.8967 indicates that there is also a reasonable correlation between the lower yield strength and  $d^{-\frac{1}{2}}$ .

#### Strain Hardening Exponent

The strain hardening exponent ( $n$ ) of the hot work material as a function of fabrication temperature is shown in Figure 9. The strain hardening exponent of the cold work-hot work material is also shown in Figure 10. It should be pointed out here that it is desired to have large values of the strain hardening exponent because large values will result in stronger work hardened steels.

#### Hot Work Material

The strain hardening exponent, which is a measure of the rate of

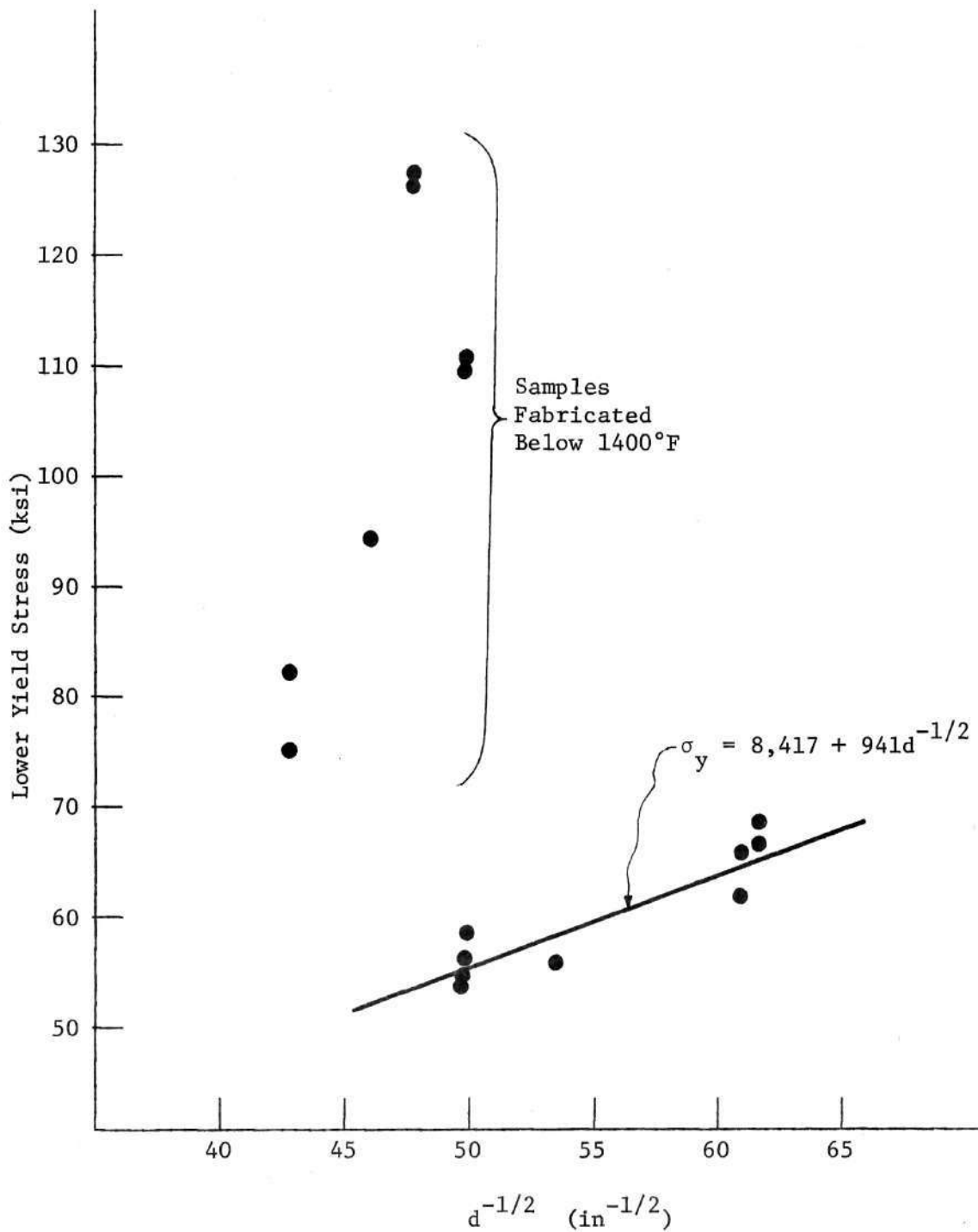


Figure 8. Applicability of the Hall-Petch Equation, Cold Work-Hot Work Longitudinal Specimens.

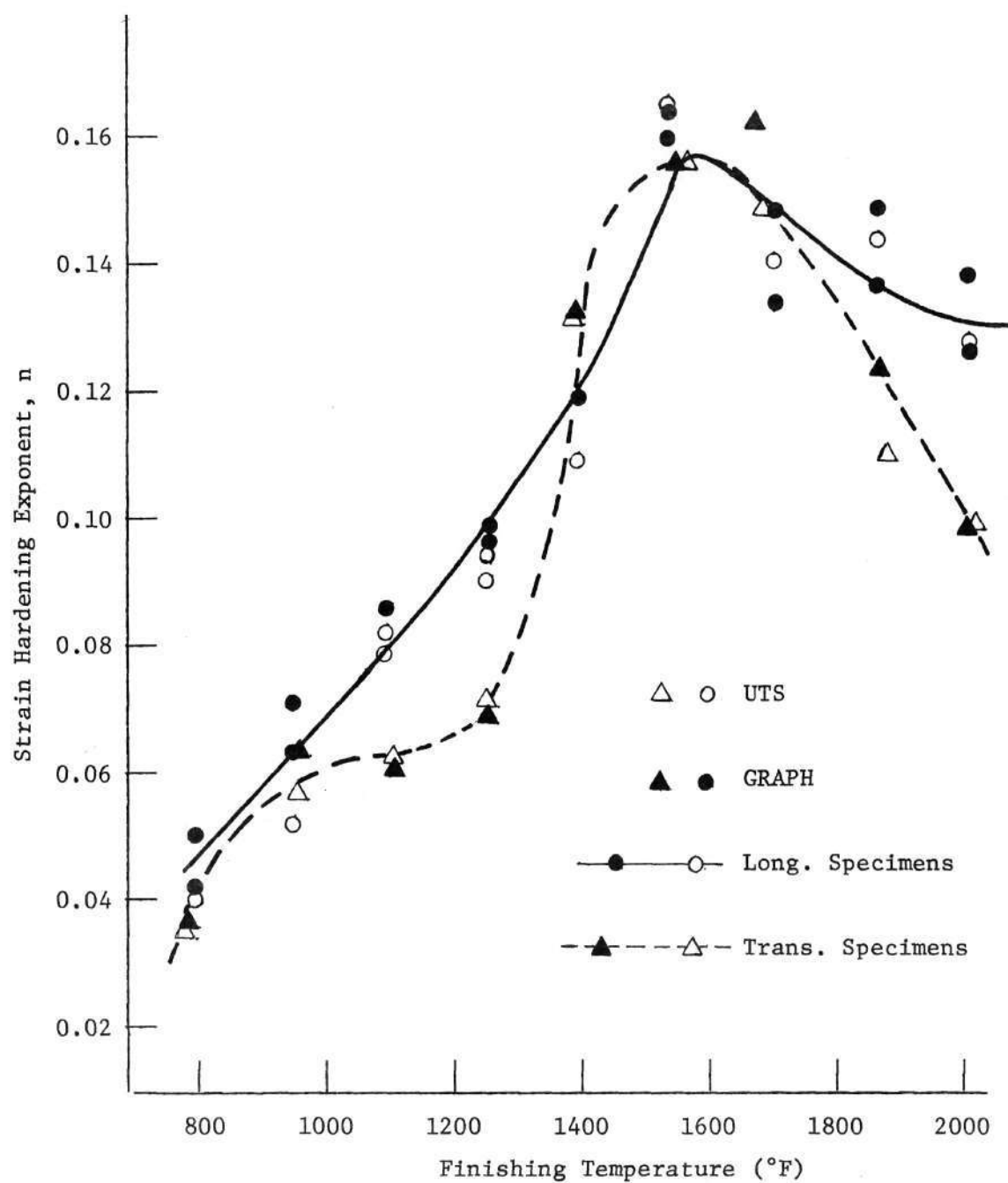


Figure 9. Strain Hardening Exponent as a Function of  
Fabrication Temperature, Hot Work Specimens.

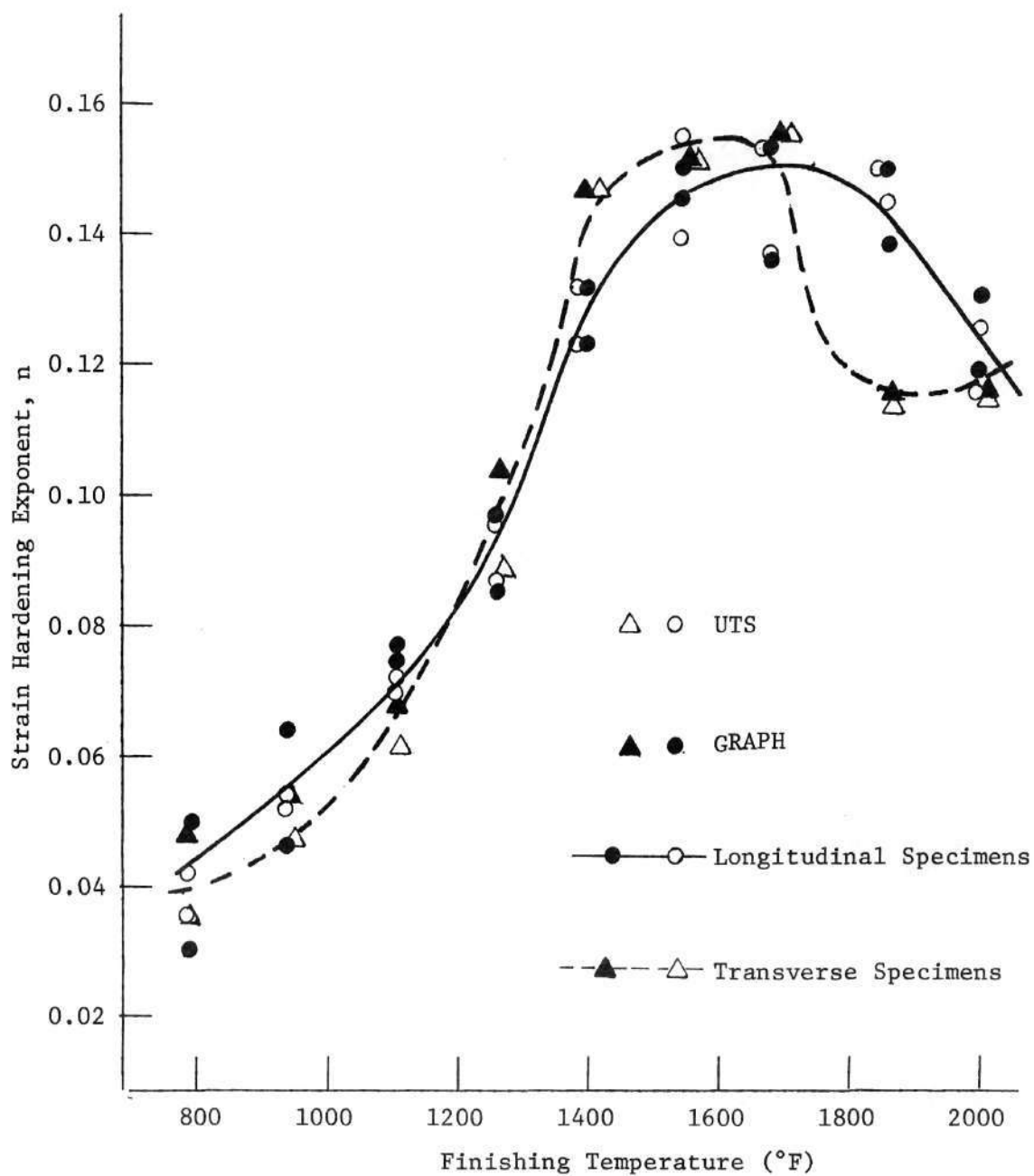


Figure 10. Strain Hardening Exponent as a Function of Fabrication Temperature, Cold Work-Hot Work Specimens.

strain hardening, increases sharply in Figure 9 from approximately 0.04 to 0.13 in the fabrication range of 800°F to 1400°F. The material at 800°F has large ferrite grains surrounding pearlite grains and the material therefore work hardens in the softer ferrite. Thus the strain hardening exponent is low. As the fabrication temperature is increased toward 1400°F, the ferrite grains surrounding the pearlite grains become smaller, and the material therefore tends to work harden against the harder pearlite. Therefore the strain hardening exponent increases. When the material is fabricated between 1400°F and 1550°F, a finer and harder microstructure increases the value of  $n$  further. As temperatures increase from 1550°F to 2000°F, the grains of ferrite will become larger (see discussion on ferrite mean intercept diameter), and the material will tend to work harden against the softer ferrite resulting in smaller values of  $n$ . The strain hardening exponents for transverse specimens have lower values than those of the longitudinal specimens in the 800°F to 1400°F range. The material is not as work hardened in the transverse direction as in the longitudinal direction. From 1400°F to 1550°F, the transverse specimen exponent values are larger than those for the longitudinal specimens. The material is probably work hardening more against the stronger pearlite which is predominant in the transverse direction. The transverse and the longitudinal values of  $n$  are approximately equal at fabrication temperatures from 1550°F to 1700°F due to the equiaxed nature of the material's grain structure (see the photomicrographs at 1550°F and 1700°F). From fabrication temperatures of 1700°F to 2000°F, the transverse values of  $n$  are less than the

longitudinal values due to mechanical fibering anisotropy in the longitudinal direction.

#### Cold Work-Hot Work Material

Figure 10 shows that in a fabrication range of  $800^{\circ}\text{F}$  to  $1400^{\circ}\text{F}$ , the strain hardening exponent values of both the transverse and the longitudinal specimens have approximately the same values in contrast to the hot work material in the same temperature range (Figure 9). The cold work-hot work material is probably more work hardened in the transverse direction due to the cold rolling. At  $1400^{\circ}\text{F}$ , the strain hardening exponent of the transverse specimens is greater than that of the longitudinal specimens because there are less ferrite grain boundaries in the transverse direction. In the temperature range of  $1550^{\circ}\text{F}$  to  $1700^{\circ}\text{F}$ , the strain hardening exponent values of the transverse and longitudinal specimens are approximately equal due to the equiaxed nature of the material's grain structure. For longitudinal specimens, the cold work-hot work specimens have exponent values which are lower than those of the hot work material in the fabrication range of  $800^{\circ}\text{F}$  to  $1250^{\circ}\text{F}$ . This is expected since the material has been preliminary cold worked. At approximately  $1300^{\circ}\text{F}$ , preliminary cold rolling seems to lose its effect due to recovery, and the values of  $n$  for both the longitudinal cold work-hot work and hot work materials are approximately the same in the fabrication range of  $1300^{\circ}\text{F}$  to  $1500^{\circ}\text{F}$ . At  $1550^{\circ}\text{F}$  the strain hardening exponent for the cold work-hot work longitudinal specimens is less than the exponent for the longitudinal hot work specimens. This is probably due to less

precipitation hardening particles in the cold work-hot work micro-structure.

#### Strength Coefficient

The strength coefficient ( $K$ ) of the hot work material is plotted against the fabrication temperature in Figure 11. The strength coefficient of the cold work-hot work material is also shown in Figure 12. It should be pointed out here that large values of strength coefficients are an indication of strong microstructures.

#### Hot Work Material

In Figure 11, the strength coefficient decreases from a fabrication temperature of  $800^{\circ}\text{F}$  to an approximate temperature of  $1400^{\circ}\text{F}$  ( $1250^{\circ}\text{F}$  for the transverse specimens). The microstructures of this material lose its strengthening effects due to decreasing dislocation densities with increasing fabrication temperature. In a temperature range of  $1400^{\circ}\text{F}$  to  $1500^{\circ}\text{F}$ , the strength coefficient increases as a possible result of precipitation hardening effects. From temperature values of  $1550^{\circ}\text{F}$  to  $2000^{\circ}\text{F}$ , the values of  $K$  decrease as a result of increasing ferrite grain growth (see discussion on ferrite mean intercept diameter). In a temperature range of  $800^{\circ}\text{F}$  to  $1400^{\circ}\text{F}$ , the values of  $K$  for the transverse specimens are less than those for the longitudinal specimens. The microstructure in this fabrication range probably has less dislocation densities in the transverse direction than in the longitudinal direction. For temperatures of  $1400^{\circ}\text{F}$  to  $1700^{\circ}\text{F}$ , the values of  $K$  for both the transverse and longitudinal specimens are approximately equal due to the

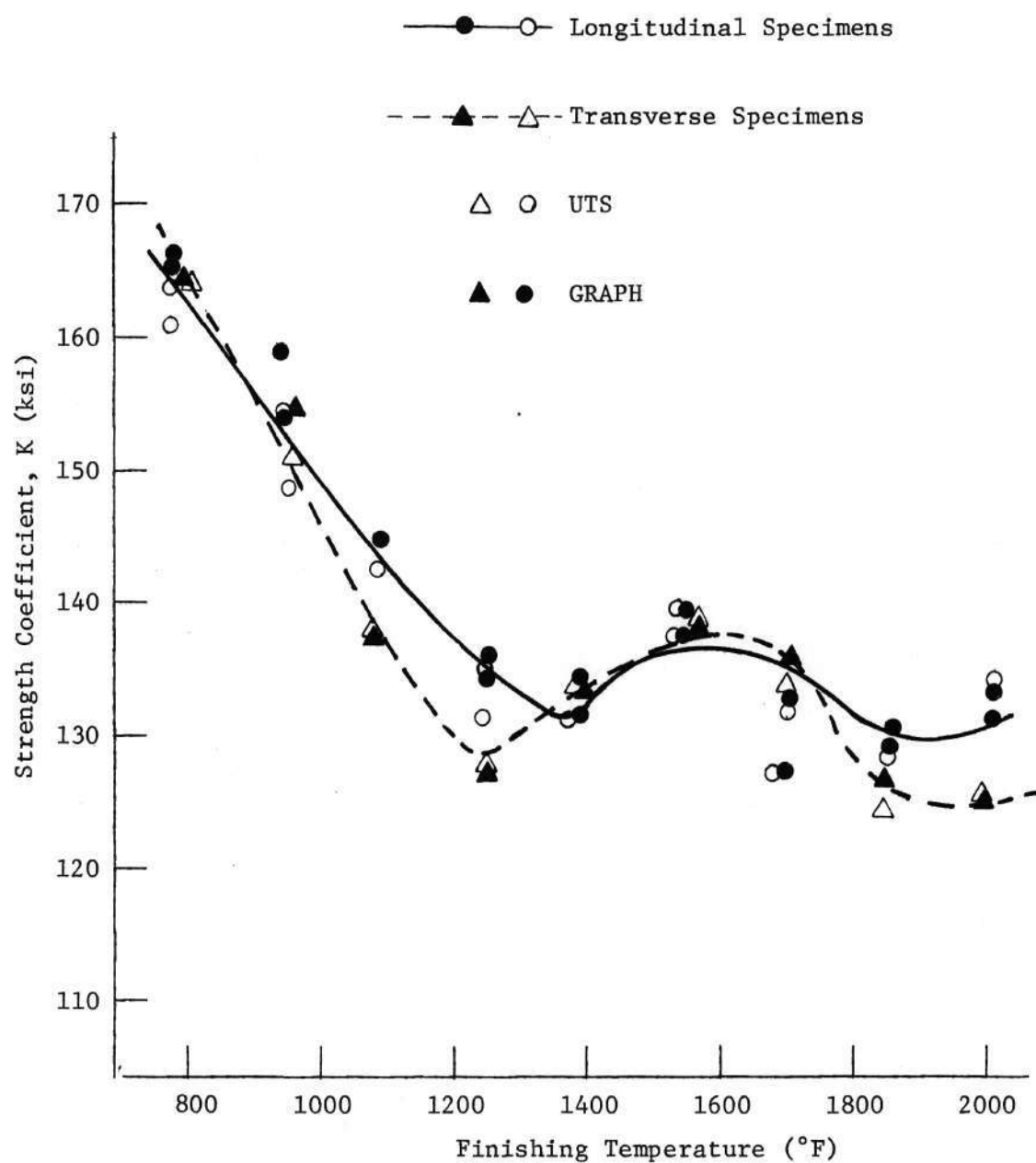


Figure 11. Strength Coefficient as a Function of  
Fabrication Temperature, Hot Work Specimens.

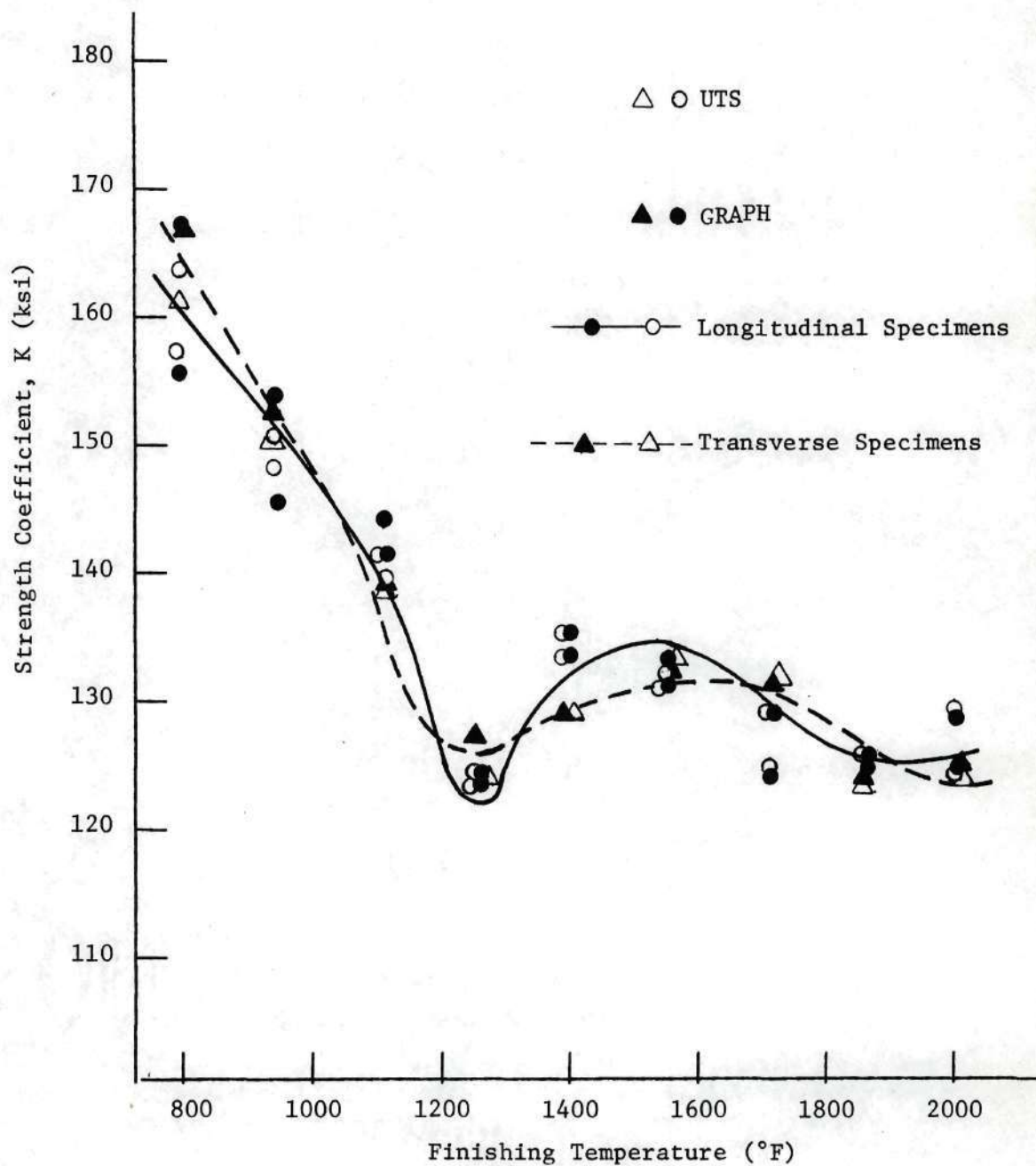


Figure 12. Strength Coefficient as a Function of Fabrication Temperature, Cold Work-Hot Work Specimens.

equiaxed nature of the material's microstructure (see the photomicrographs at 1400°F, 1550°F, and 1700°F). From fabrication temperatures of 1700°F to 2000°F, the transverse K values decrease from the K values of the longitudinal specimens because there is probably mechanical fibering anisotropy in the longitudinal direction.

#### Cold Work-Hot Work Material

From Figure 12, it is seen that the transverse strength coefficient values are not much different from those of the longitudinal specimens. In the temperature range of 800°F to 1100°F, the strength coefficients of the hot work material (Figure 11) and the cold work-hot work material are approximately the same. At 1250°F, the strength coefficient values of the cold work-hot work longitudinal specimens are considerably lower than the values of the hot work longitudinal specimens, and preliminary cold rolling seems to have lost its effect. In the temperature range of 1400°F to 2000°F, the strength values of the cold work-hot work material are less than the values of the hot work material. This is probably due to less precipitation hardening particles in the cold work-hot work microstructure than there are in the hot work microstructure.

#### Per Cent Elongation (Ductility)

The total per cent elongation (ductility) of the hot work material is plotted against the fabrication temperature in Figure 13. The per cent elongation of the cold work-hot work material is also plotted in Figure 14.

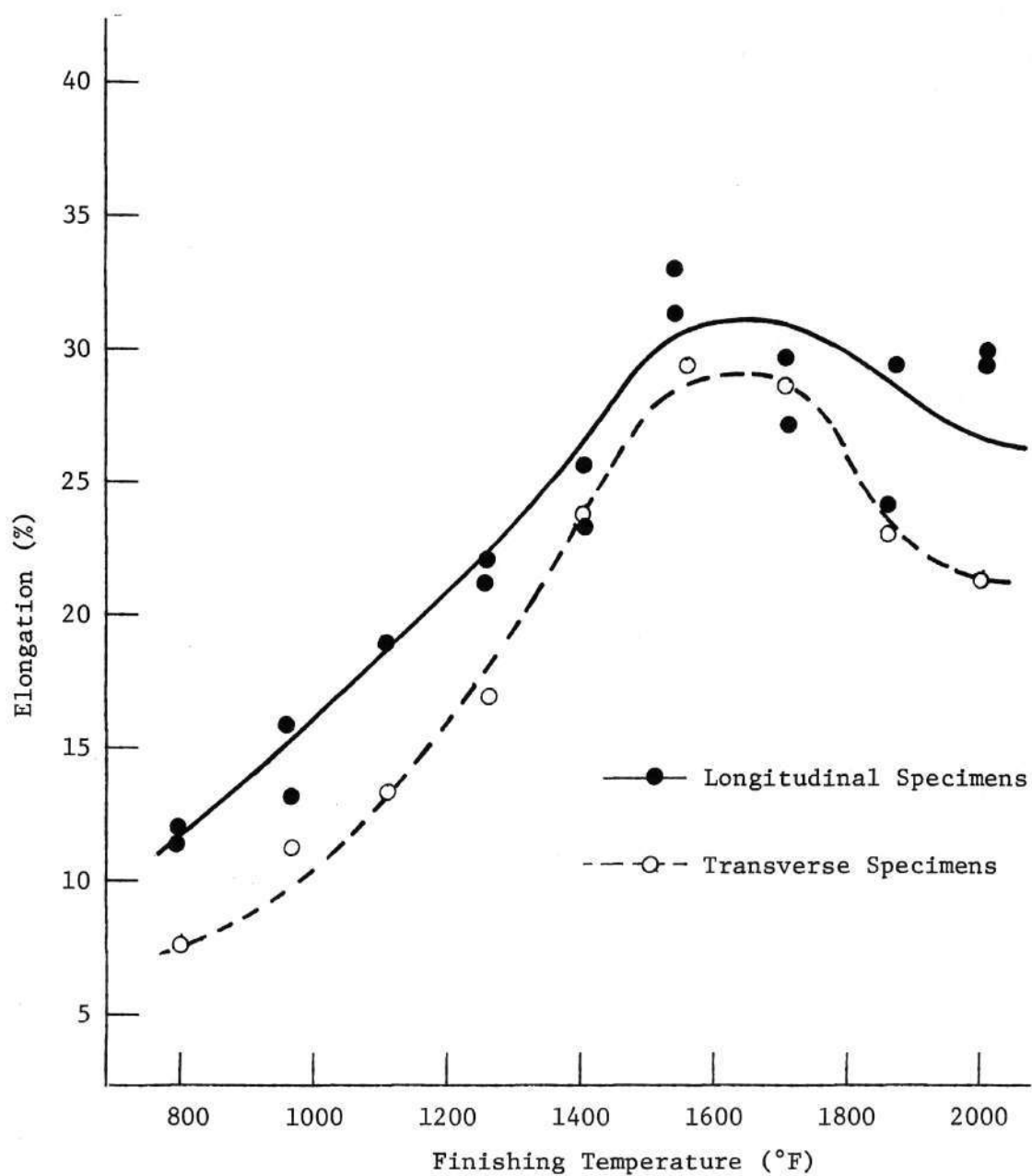


Figure 13. Percent Elongation as a Function of  
Fabrication Temperature, Hot Work Specimens.

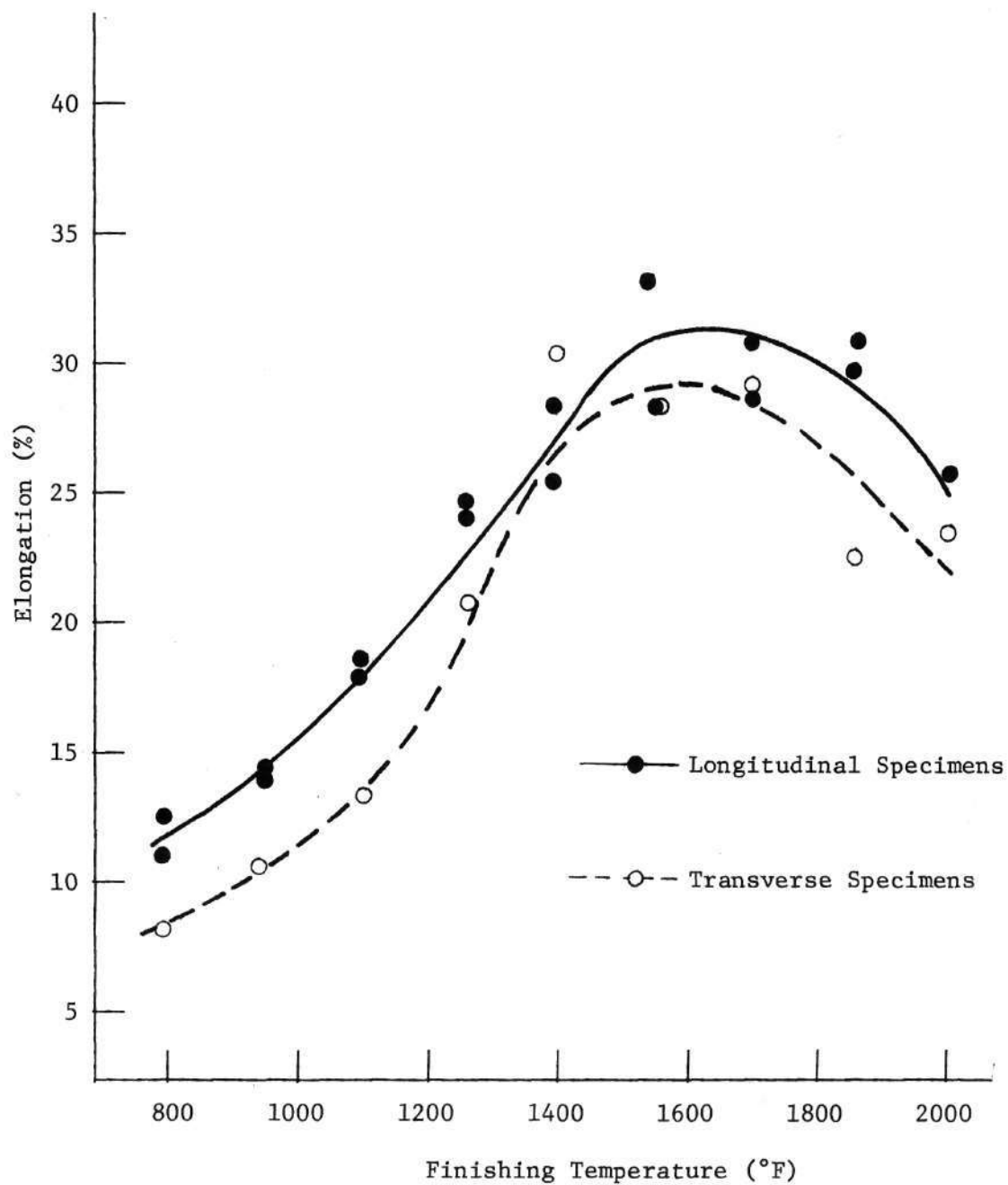


Figure 14. Percent Elongation as a Function of Fabrication Temperature, Cold Work-Hot Work Specimens.

### Hot Work Material

The per cent elongation (ductility) in Figure 13 increases in the fabrication range of 800°F to approximately 1600°F as a result of decreasing dislocation density in the microstructure with increasing fabrication temperature. As the fabrication temperature is increased beyond 1600°F, the ductility appears to decrease with increasing grain size (see discussion on ferrite mean intercept diameter). The transverse specimens have lower elongation values than those of the longitudinal specimens because there are fewer grain boundaries in the transverse direction.

### Cold Work-Hot Work Material

Figure 14 indicates that the ductility of the cold work-hot work material has the same behavior as the ductility of the hot work material (Figure 13). Preliminary cold working appears to have little effect on the ductility of X-60 steel. Ductility seems to be more dependent on fabrication temperature.

### V-Notch Charpy Transition Temperature

The V-notch Charpy transition temperatures of the hot work material are plotted against the fabrication temperatures in Figure 15. The Charpy transition temperatures of the cold work-hot work material are also shown in Figure 15.

### Hot Work Material

In a fabrication temperature range of 800°F to 1250°F, Figure 15 shows that the transition temperature of the hot work material is unusually high because of the work hardening effects and the large grain sizes (see the discussion on ferrite mean intercept diameter).

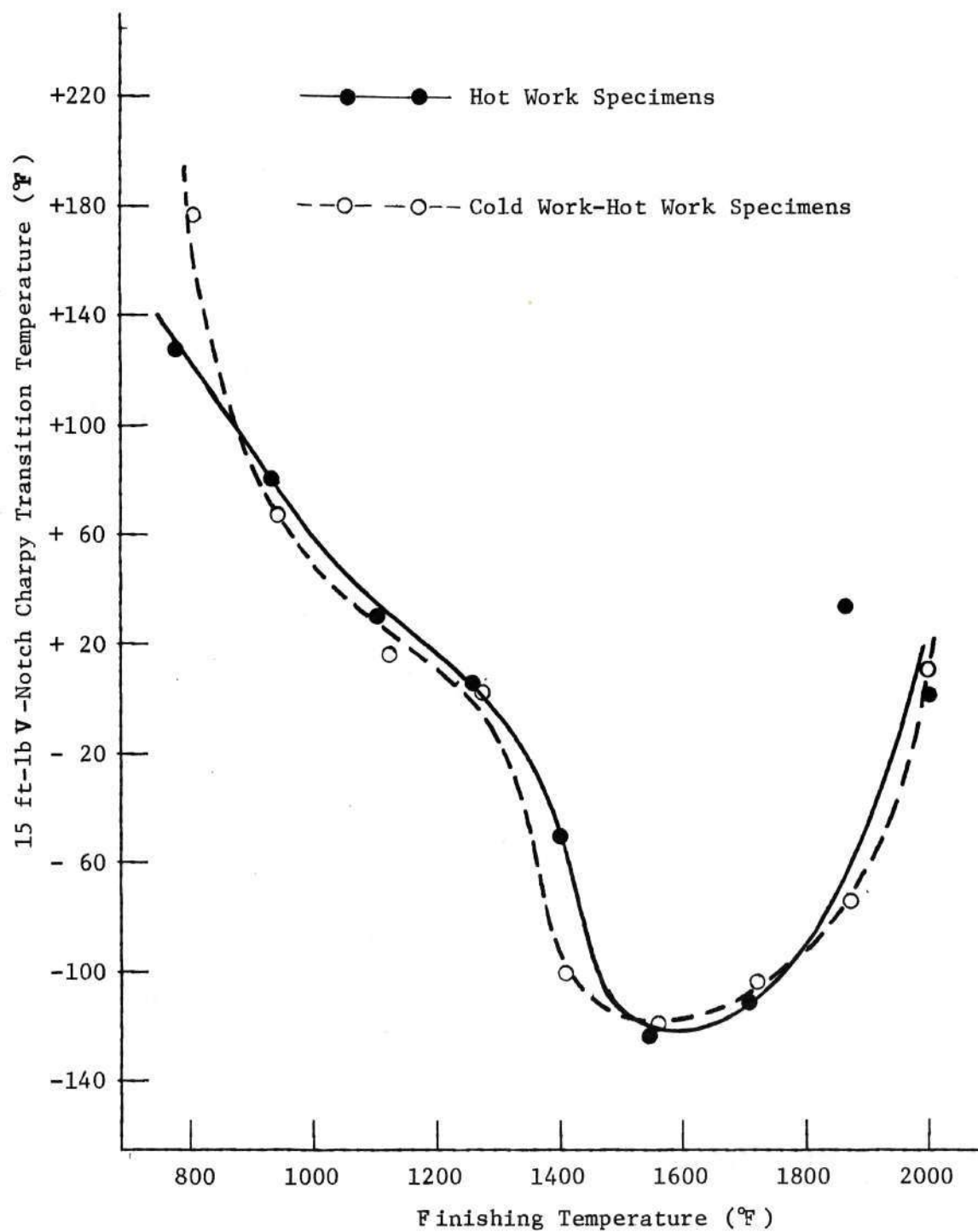


Figure 15. V-Notch Charpy Transition Temperature as a Function of Fabrication Temperature.

As the fabrication temperature decreases to  $1550^{\circ}\text{F}$ , the transition temperature reaches a minimum as a result of a finer grain structure and of the disappearance of the work hardening effects. Increasing the fabrication temperature above  $1550^{\circ}\text{F}$  yields larger grain structures resulting in a decrease in the Charpy transition temperature.

#### Cold Work-Hot Work Material

In a fabrication temperature range of  $950^{\circ}\text{F}$  to  $1400^{\circ}\text{F}$ , Figure 15 shows that the Charpy transition temperatures of the cold work-hot work material are less than the transition temperatures of the hot work material in the same temperature range. It appears that preliminary cold rolling improves the energy absorbing capacity of the steel especially at a fabrication temperature of  $1400^{\circ}\text{F}$ . At a fabrication temperature of  $1550^{\circ}\text{F}$ , the transition temperature is a minimum and is slightly higher than the corresponding hot work material.

#### Ferrite Orientation Factor

The ferrite orientation factor of the hot work material is plotted against the fabrication temperature in Figure 16. The ferrite orientation factor of the cold work-hot work material is also shown in Figure 16.

#### Hot Work Material

The ferrite orientation factor of the hot work material in Figure 16 has high values in the temperature range of  $800^{\circ}\text{F}$  to  $1400^{\circ}\text{F}$ . This is expected since the grains are elongated by work hardening

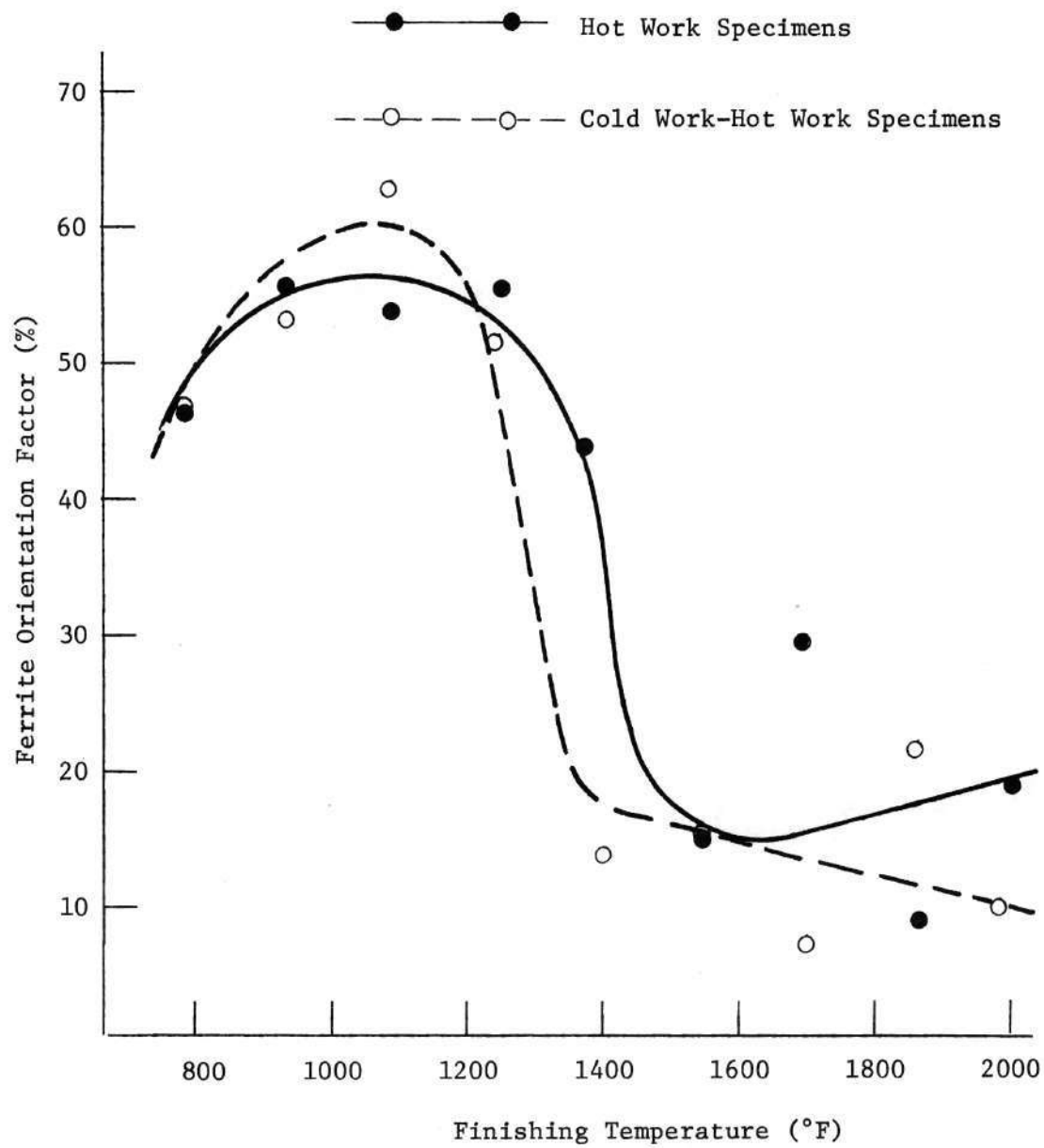


Figure 16. Ferrite Orientation Factor as a Function of Fabrication Temperature.

effects in the rolling direction. At fabrication temperatures above  $1400^{\circ}\text{F}$ , the grains lose their work hardening effects and tend to become more equiaxed, thus resulting in lower ferrite orientation factor values.

#### Cold Work-Hot Work Material

Figure 16 shows that the behavior of the ferrite orientation factor of the cold work-hot work material is approximately the same as that of the hot work material. In the temperature range of  $800^{\circ}\text{F}$  to  $1200^{\circ}\text{F}$ , the orientation factors are equal to or more than the factors for the hot work material. At approximately  $1200^{\circ}\text{F}$ , the cold work-hot work material seems to lose its cold work effects due to recovery, and the material has orientation factor values less than those for the hot work material in the fabrication temperature range of  $1200^{\circ}\text{F}$  to  $1550^{\circ}\text{F}$ . At  $1550^{\circ}\text{F}$ , the orientation factor values for both the hot work and the cold work-hot work materials have approximately the same values due to the small and equiaxed microstructure of both materials.

#### Ferrite Mean Intercept Diameter

The ferrite mean intercept diameter of the hot work material is plotted against the fabrication temperature in Figure 17. The ferrite mean intercept diameter of the cold work-hot work material is also shown in Figure 17.

#### Hot Work Material

In a fabrication temperature range of  $800^{\circ}\text{F}$  to  $1250^{\circ}\text{F}$ , Figure 17 shows that the ferrite grain diameter of the hot work material is relatively constant. From  $1400^{\circ}\text{F}$  to  $1550^{\circ}\text{F}$ , the material is heated in the ferrite-austenite region, and the ferrite has little time for

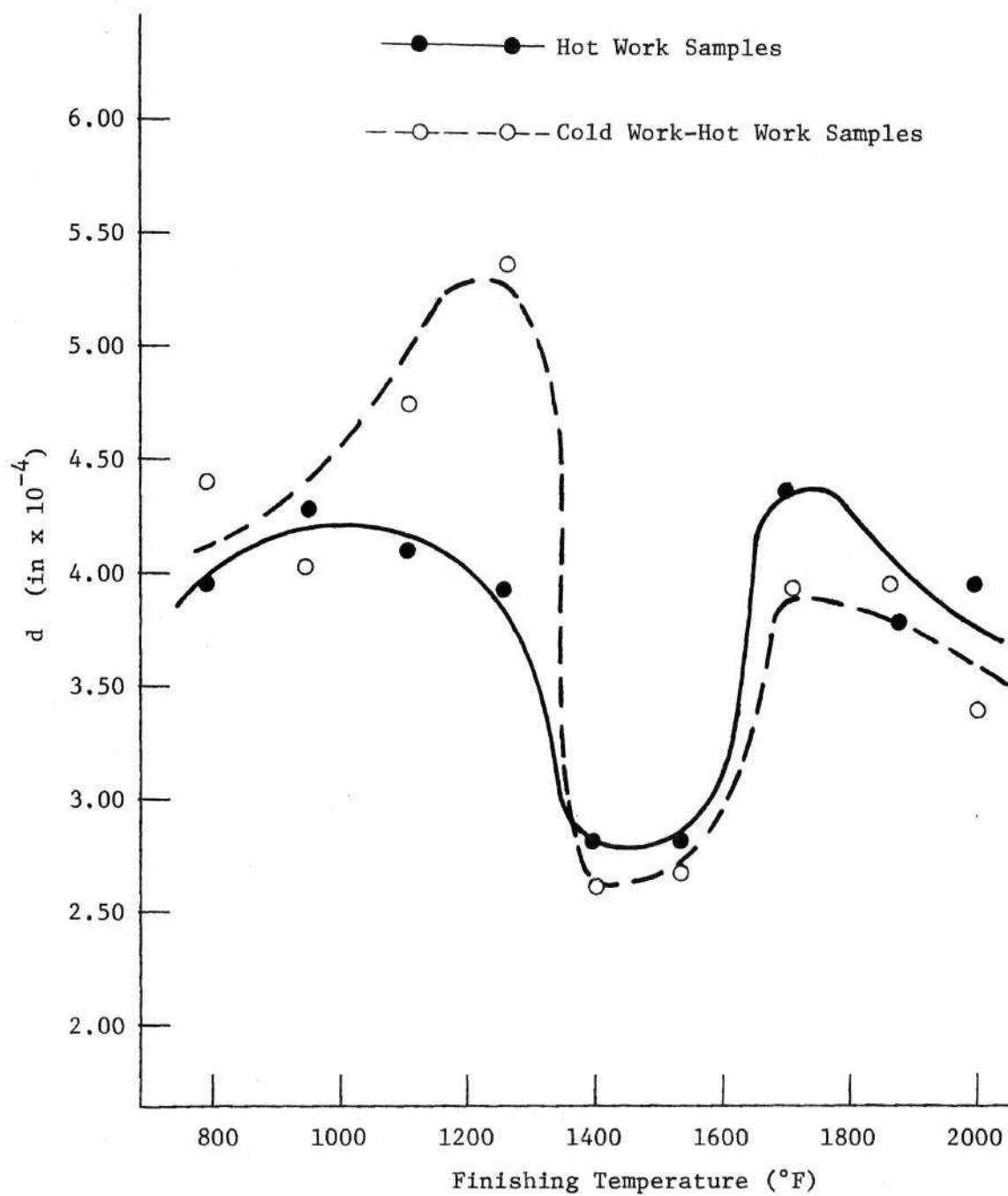


Figure 17. Ferrite Mean Intercept Diameter ( $d$ ) as a Function of Fabrication Temperature.

grain growth. The ferrite grain diameter is therefore considerably smaller. In the temperature range of  $1550^{\circ}\text{F}$  to  $1700^{\circ}\text{F}$ , the ferrite grain diameter increases considerably due to the increased ferrite growth time. From  $1700^{\circ}\text{F}$  to  $2000^{\circ}\text{F}$ , the ferrite diameter decreases somewhat.

#### Cold Work-Hot Work Material

From a fabrication temperature range of  $800^{\circ}\text{F}$  to  $1350^{\circ}\text{F}$ , Figure 17 shows that preliminary cold rolling produces larger ferrite grain diameters than those of the hot work material. As the fabrication temperature increases beyond  $1350^{\circ}\text{F}$ , the grain diameter values tend to become smaller as compared to those of the hot work material. This phenomenon is due to the slower rate of ferrite recrystallization which is caused by preliminary cold rolling.

#### Comparison of Results

Mechanical properties of both the hot work material and the cold work-hot work material in a fabrication range of  $1400^{\circ}\text{F}$  to  $1700^{\circ}\text{F}$  are compared in Figures 18 to 21. These properties of the mill material are also shown in these figures. The fabrication temperature range of  $1400^{\circ}\text{F}$  to  $1700^{\circ}\text{F}$  was chosen for the comparison because it was observed that the strain hardening exponent (Figures 9 and 10) and ductility (Figures 13 and 14) both had its highest values in this temperature range. This temperature range also corresponded to the lowest values of the Charpy transition temperature (Figure 15). The bars at each fabrication treatment, shown in Figures 18 to 21, incorporate both longitudinal and transverse specimen data where

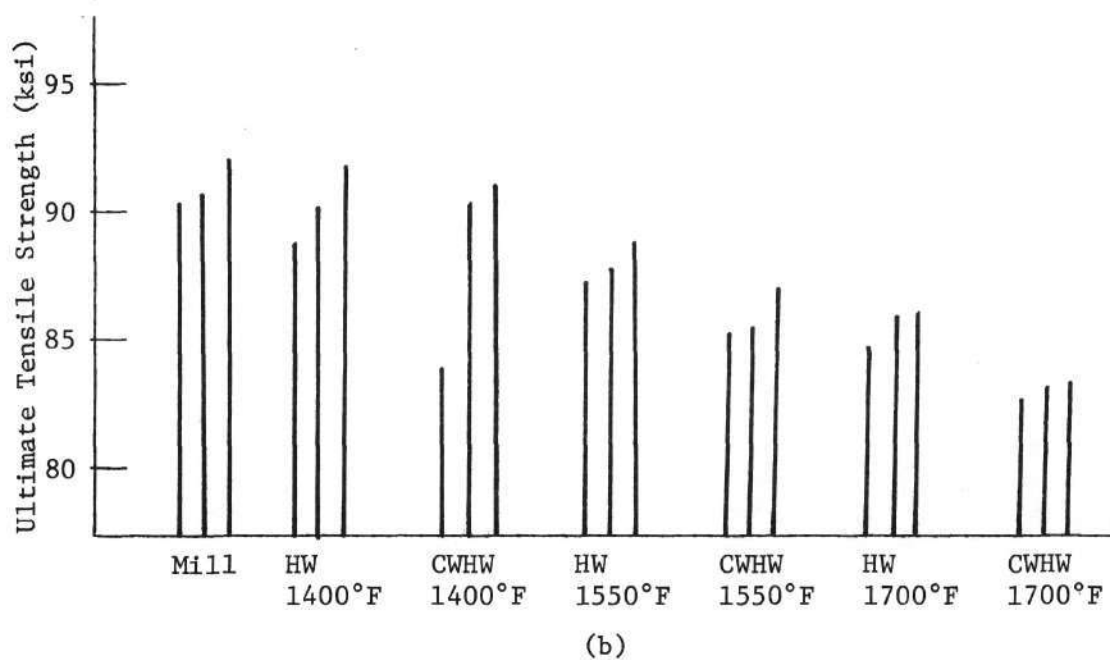
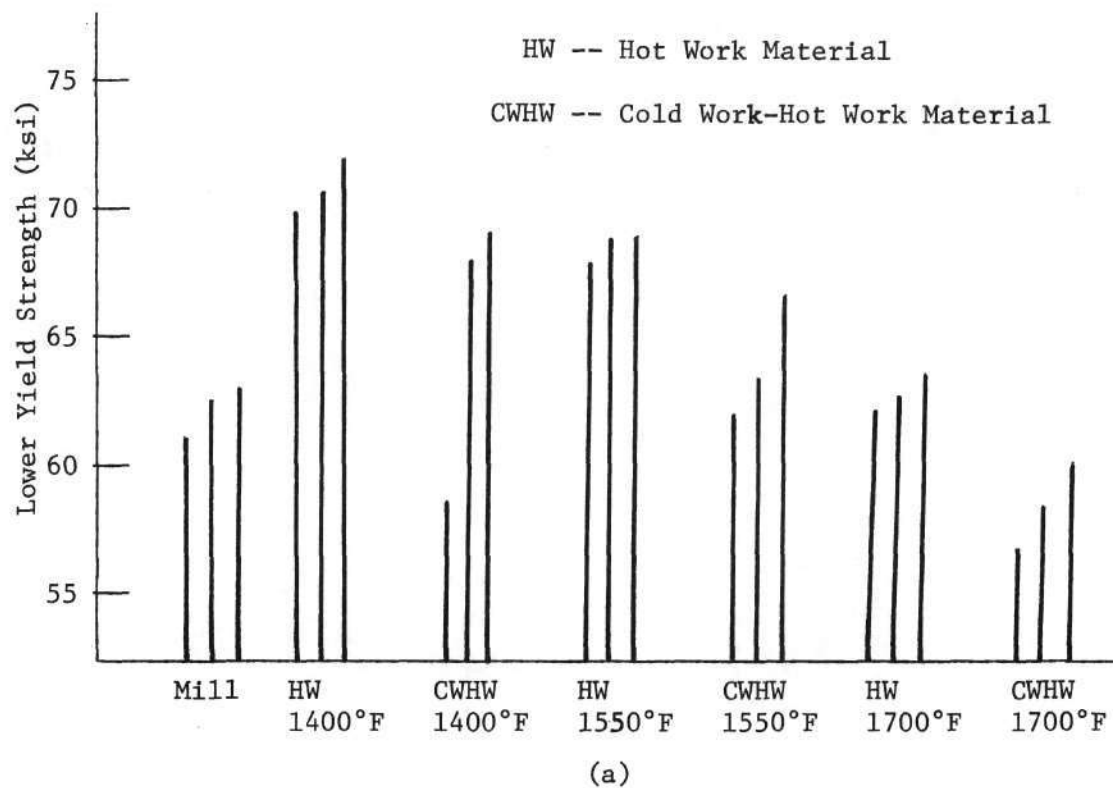


Figure 18. Comparison of Lower Yield Strengths and Ultimate Tensile Strengths.

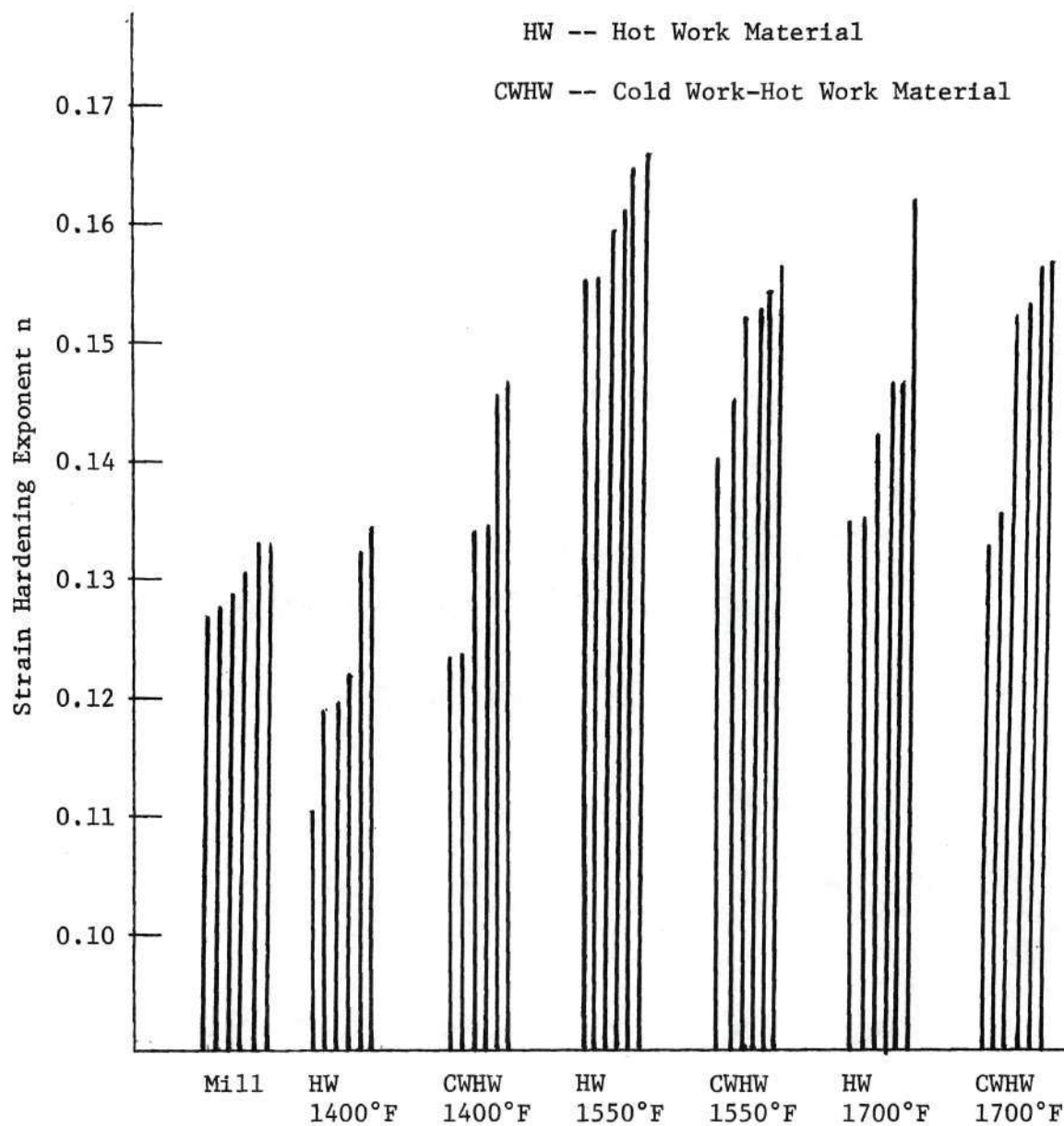


Figure 19. Comparison of Strain Hardening Exponents ( $n$ ).

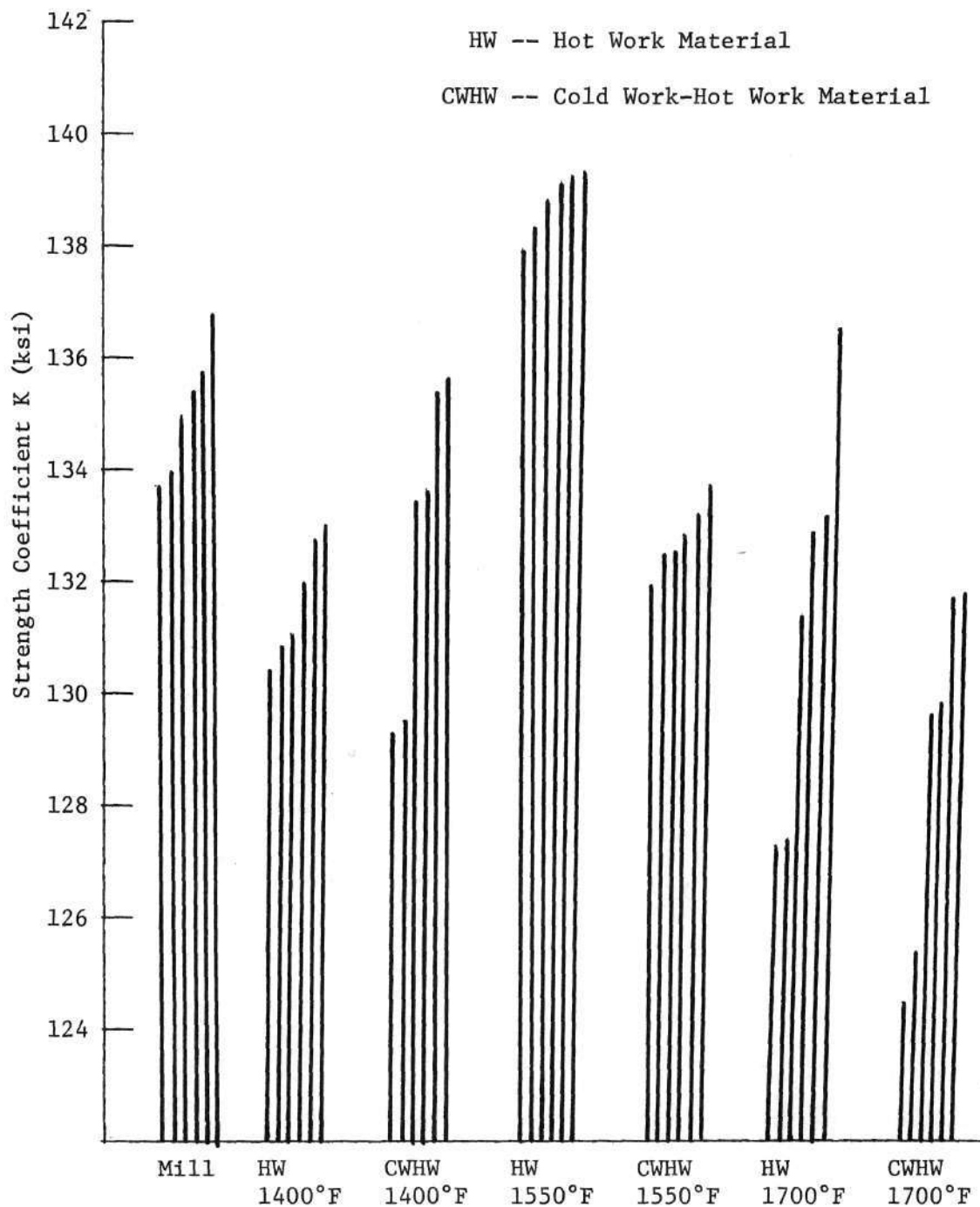


Figure 20. Comparison of Strength Coefficients (K).

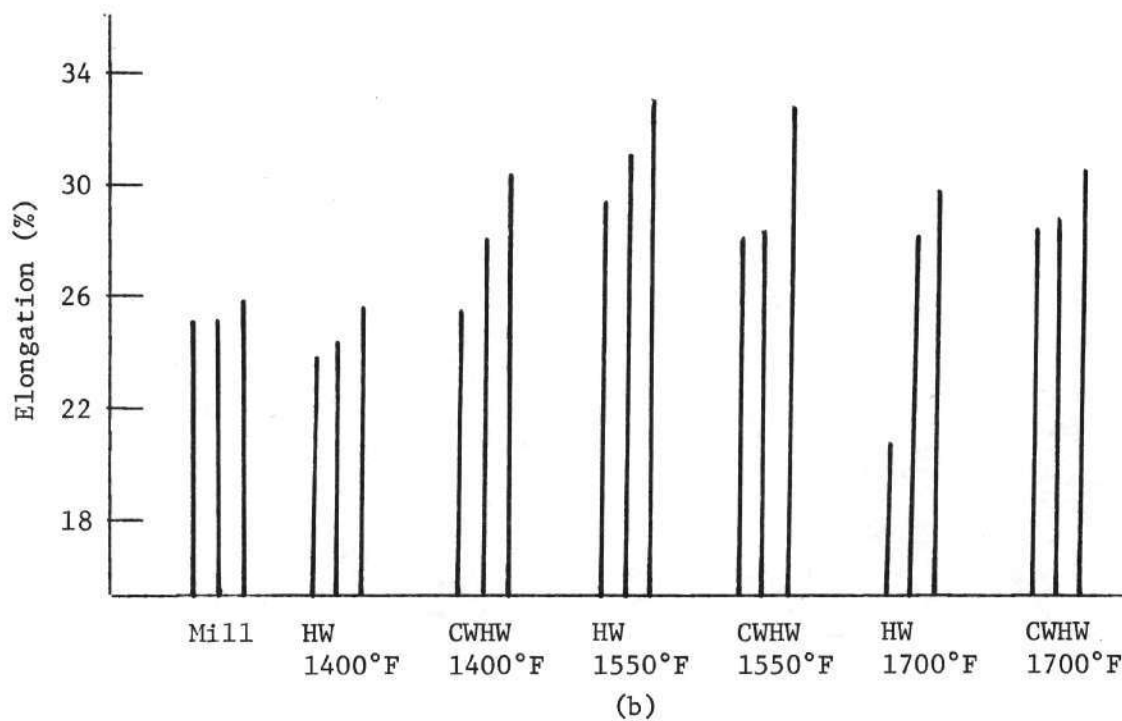
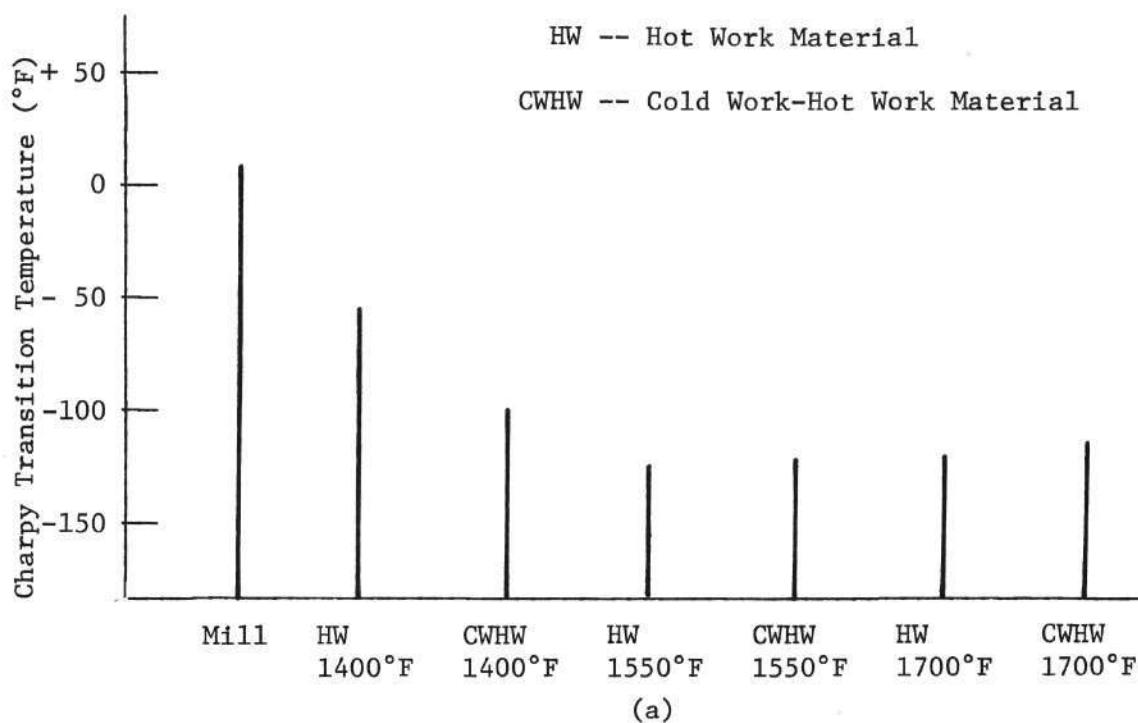


Figure 21. Comparison of Charpy Transition Temperatures and Ductilities (Total Percent Elongation).

applicable.

The lower yield strength is shown in Figure 18(a). The hot work material at 1400°F shows the largest values of lower yield stress while the hot work material at 1550°F shows slightly lower values. The lower yield strength at 1550°F hot work fabrication is 5,000 to 6,000 psi more than the lower yield strength of the material in the mill condition. The ultimate yield strength, which is also shown in Figure 18(b), has its maximum values when the X-60 steel is in the mill condition.

The strain hardening exponent ( $n$ ) is shown in Figure 19. The values of the strain hardening exponent at 1550°F hot work fabrication is a maximum and has an increase of approximately 0.03 over those values for the mill condition.

The hot work treatment at 1550°F yields large values of the strength coefficient as shown in Figure 20. Although larger values of the strength coefficient result at fabrication processes below 1400°F, the strength coefficient values at 1550°F hot work fabrication are a maximum for the temperature range indicated in the figure. These are approximately 3,000 to 4,000 psi more than values for the mill condition.

Figure 21(a) shows that the 15 ft-lb Charpy transition temperature at 1550°F hot work fabrication is a minimum at -122°F. The Charpy transition temperature of the mill material is +9°F. Figure 21(b) also shows that the ductility is a maximum at 1550°F hot work fabrication and that it is improved by 6 to 8 per cent when compared to the material in the mill condition.

It is seen from the figures that the hot work material fabricated at 1550°F yields the optimum combination of mechanical properties when this material is compared to the material in the mill condition. These figures also indicate that preliminary cold working is not beneficial to yielding an optimum combination of mechanical properties.

#### Photomicrographs

Some microstructures of the X-60 hot work materials are shown in this section of the text. In Figure 22 the material fabricated at 950°F is shown. The work hardening effects are evident because of the elongated grain structures in the rolling direction. Figure 23 shows a fine microstructure with many pearlite grains orientated in the rolling direction. This material was fabricated at a temperature of 1400°F which was probably close to the eutectoid temperature. It can be concluded that this microstructure is a result of an isoforming process. In Figure 24 the material was fabricated at 1550°F resulting in a fine equiaxed grain structure. The ferrite grains had little time to grow which indicates that this material was fabricated near the austenite-ferrite transformation temperature. Figure 25 shows the material fabricated at 1700°F. This temperature was above the transformation temperature, and thus larger ferrite grains resulted. In Figure 26 the material fabricated at 2000°F is shown. The large ferrite grain structure is the result of a longer recrystallization process.

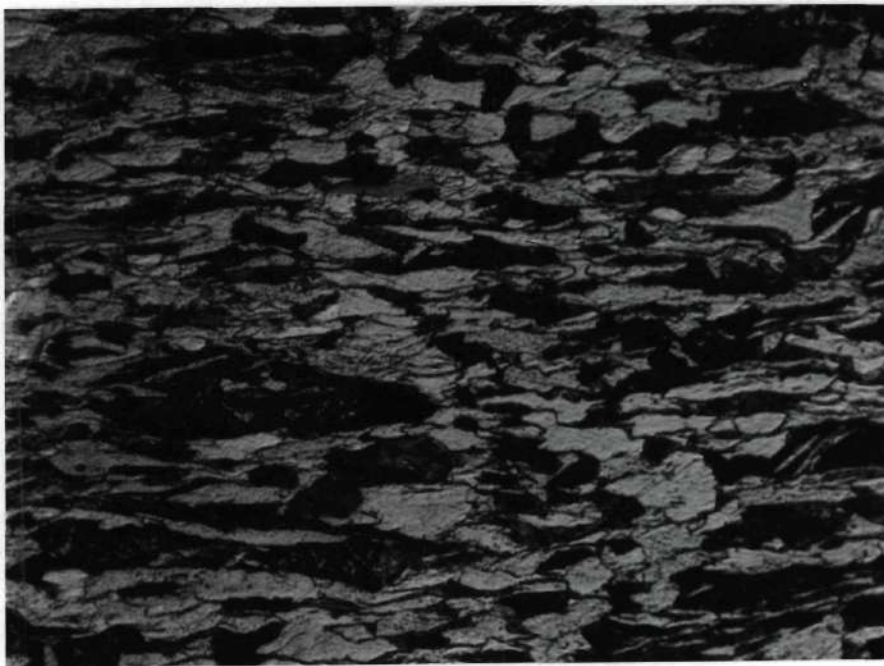


Figure 22. Photomicrograph of the Hot Work Material at  
950°F Fabrication, Magnification 400x.

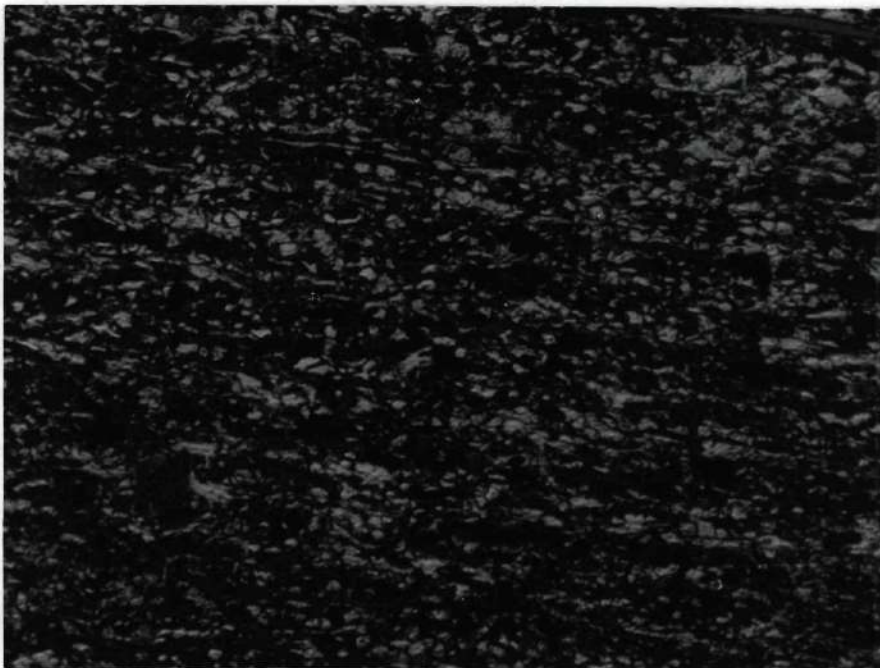


Figure 23. Photomicrograph of the Hot Work Material at  
1400°F Fabrication, Magnification 400x.

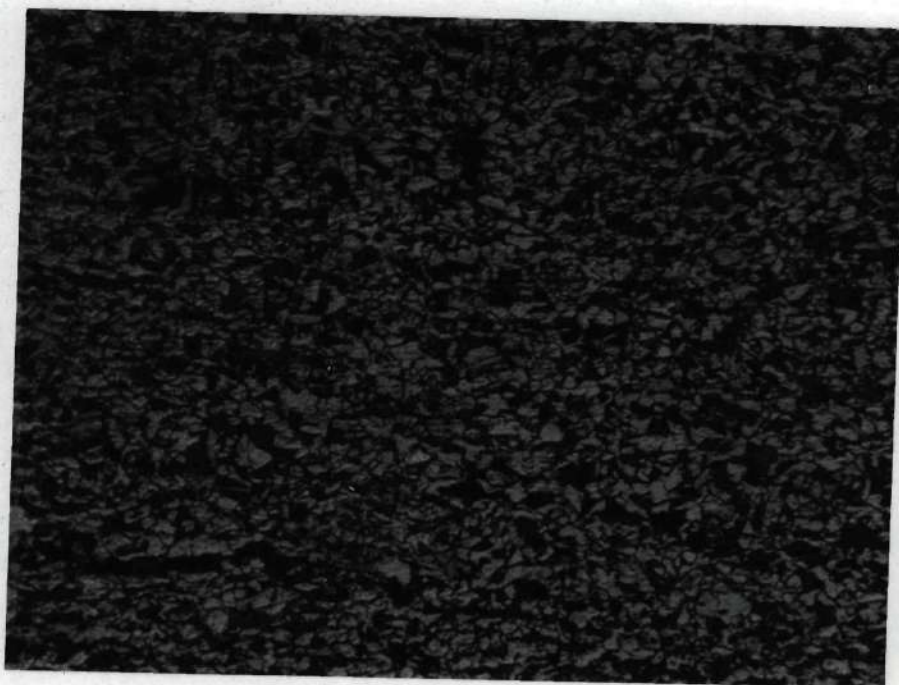


Figure 24. Photomicrograph of the Hot Work Material at  
1550°F Fabrication, Magnification 400x.

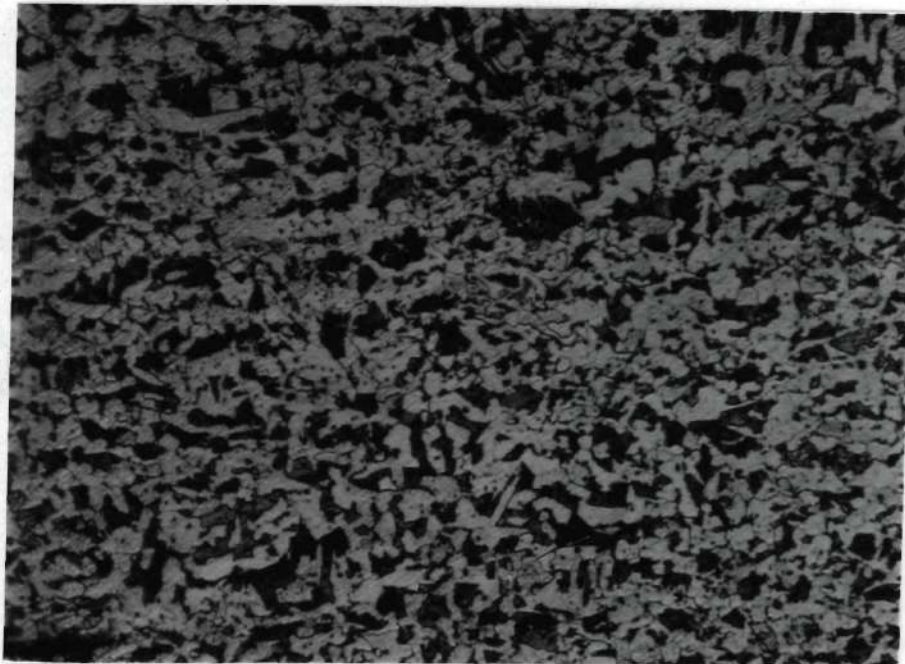


Figure 25. Photomicrograph of the Hot Work Material at  
1700°F Fabrication, Magnification 400x.

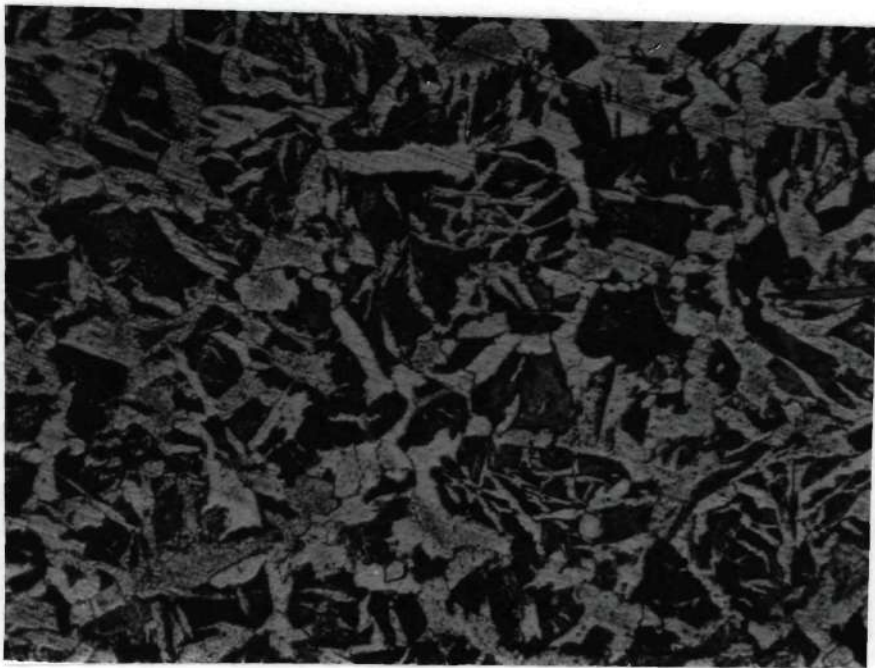


Figure 26. Photomicrograph of the Hot Work Material at  
2000°F Fabrication, Magnification 400x.

## CHAPTER VI

## CONCLUSIONS

It is concluded from the results that the hot work material fabricated at  $1550^{\circ}\text{F}$  gives an optimum combination of mechanical properties when these properties are compared to the mechanical properties of the material in the mill conditions. The mill condition can be thought of as representing the usual heat treatment of X-60 steel when it is prepared for commercial use. The  $1550^{\circ}\text{F}$  hot work fabrication of the X-60 steel yields the maximum possible values of both the strain hardening exponent and the total per cent elongation (ductility). The Charpy transition temperature has its lowest possible value at the  $1550^{\circ}\text{F}$  hot work fabrication. Both the lower yield strength and the strength coefficient at the  $1550^{\circ}\text{F}$  hot work fabrication show higher values than those values of the mill material. Thus hot rolling at  $1550^{\circ}\text{F}$  (high temperature thermomechanical treatment - HTTMT) is the appropriate fabrication treatment for X-60 steel.

It is concluded that preliminary cold rolling (preliminary thermomechanical treatment - PTMT) of the X-60 steel is not beneficial to yielding an optimum combination of mechanical properties. It was observed in the discussion for some of the mechanical properties of the cold work-hot work material that preliminary cold rolling seems to lose its effect in the approximate fabrication temperature range

of 1200°F to 1300°F.

It is also concluded that the Hall-Petch relationship seems to apply for both the hot work and the cold work-hot work X-60 steel. Linear regression analysis indicated that there is a reasonable correlation between the lower yield strength and  $d^{-\frac{1}{2}}$ .

## BIBLIOGRAPHY

1. Koppenaal, T. J., "The Current Status of Thermomechanical Treatment in the Soviet Union," Transactions ASM, Vol. 62, pp. 24, 1968.
2. Latham, D. J., "The Current Position of Thermomechanical Treatment Applied to Engineering and Tool Steels," Journal of the Iron and Steel Institute, Vol. 208, pp. 50, 1970.
3. Ivanova, V. S., and L. K. Gordienko, "New Ways of Increasing the Strength of Metals," Iron and Steel Institute Publication 109, 1968.
4. Cryderman, R. L., A. P. Coldren, J. R. Bell, and J. D. Grozier, "Controlled-Cooled Structural Steels Modified with Columbium, Molybdenum, and Boron," Transactions ASM, Vol. 62, pp. 561, 1969.
5. Yeo, R. B. G., A. G. Melville, P. E. Repas, and J. M. Gray, "Properties and Control of Hot Rolled Steel," Journal of Metals, Vol. 20, pp. 33, 1968.
6. Irani, J. J., and D. J. Latham, "Applications of Isoforming and Applied Treatments to Low Alloy Steels," Iron and Steel Institute Publication 114, pp. 55, 1969.
7. MacDonald, J. K., Ship Structure Committee Report SSC-73, November, 1953.
8. Banta, H. M., R. H. Frazier, and C. H. Lorig, "Some Metallurgical Aspects of Ship Steel Quality," Welding Journal Research Supplement, Vol. 30, pp. 79s, 1951.
9. De Kazinczy, F., and W. A. Backofen, "Influence of Hot Rolling Conditions on Brittle Fracture in Steel Plate," Transactions ASM, Vol. 53, pp. 55, 1961.
10. Mackenzie, I. M., "Niobium Treated Carbon Steels," Journal of the West of Scotland Iron and Steel Institute, Vol. 60, pp. 244, 1963.
11. Biggs, W. D., Brittle Fracture of Steel, MacDonald and Evans, London, 1960.
12. Duckworth, W. E., "Metallurgy of Structural Steels: Present and Future Possibilities," Iron and Steel Institute Publication 104, pp. 61, 1967.

13. Pickering, F. B., "Precipitation of Intermetallic Compounds in Ferritic Steels," Iron and Steel Institute Publication 114, p. 131, 1969.
14. Smith, R. P., "The Solubility of Niobium (Columbium) Carbide in Gamma Iron," Transactions AIME, Vol. 236, pp. 220, 1966.
15. Smith, R. P., "The Solubility of Columbium Nitride in Gamma Iron," Transactions AIME, Vol. 224, pp. 190, 1962.
16. Gray, J. M., and R. B. G. Yeo, "Columbium Carbonitride Precipitation in Low Alloy Steels with Particular Emphasis on 'Precipitate-Row' Formation," Transactions ASM, Vol. 61, pp. 225, 1968.
17. Gray, J. M., D. Webster, and J. H. Woodhead, "Precipitation in Mild Steels Containing Small Additions of Niobium," Journal of the Iron and Steel Institute, Vol. 203, pp. 812, 1965.
18. Bungardt, K. K. Kind, and W. Oelsen, "The Solubility of Vanadium Carbide in Austenite," Archiv fur das Eisenhüttenwesen, Vol. 27, pp. 61, 1956.
19. Narita, K., "Trace Elements in Steel: IV, Vanadium Nitride," Nippon Kapaki Sasshi, Vol. 78, No. 705, 1957.
20. Larrabee, C. P., "Corrosion Resistance of HSLA Steels as Influenced by Composition and Environment," Corrosion, Vol. 9, pp. 259, 1953.
21. Irvine, K. J., "The Development of High Strength Structural Steels," Iron and Steel Institute Publication 104, pp. 1, 1967.
22. Meyer, L., and D. Schawinhold, "Effects of Niobium on the Properties of Plain Carbon Weldable Steel," Stahl and Eisen, Vol. 87, pp. 8, 1967.
23. Gray, J. M., R. B. G. Yeo, P. E. Rapas, and A. G. Melville, "Discussion Session III," Iron and Steel Institute Publication 104, pp. 249, 1967.
24. De Kazinsky, F., A. Axnas, and P. Pachlaitner, "Some Properties of Niobium Treated Mild Steel," Jernkantorets Annaler, Vol. 147, pp. 408, 1963.
25. Irani, J. J., D. Dulieu, and G. Tither, "Role of Copper in Low Alloy Steels," Iron and Steel Institute Publication 114, pp. 75, 1969.

26. Stephenson, E. T., G. H. Karchner, and P. Stark, "Strengthening Mechanisms in Mn-V-N Steels," Transactions ASM, Vol. 57, pp. 208, 1964.
27. Morrison, W. B., "The Influence of Small Niobium Additions on the Properties of Carbon-Manganese Steels," Journal of the Iron and Steel Institute, Vol. 201, pp. 437, 1963.
28. Hall, E. O., "The Deformation and Aging of Mild Steel," Proceedings of the Physical Society, Vol. B64, pp. 747, 1951.
29. Petch, N. J., "The Cleavage Strength of Polycrystals," Journal of the Iron and Steel Institute, Vol. 174, pp. 25, 1953.
30. Pickering, F. B., and T. Gladman, "Metallurgical Developments in Carbon Steels," British Iron and Steel Research Association Report 81, pp. 9, 1963.
31. Pickering, F. B., "Some Aspects of the Relationship Between Microstructure and Mechanical Properties," Iron and Steel, Vol. 38, pp. 110, 1965.
32. Jamieson, R. M., and J. W. Thomas, "Controlled Rolling of High Strength Skelp for the Manufacture of Large OD Pipe," Iron and Steel Institute Publication 104, pp. 167, 1967.
33. Duckworth, W. E., and J. D. Baird, "Mild Steel," Journal of the Iron and Steel Institute, Vol. 207, pp. 854, 1969.
34. Irvine, K. J., "Physical Metallurgy," Journal of the Iron and Steel Institute, Vol. 207, pp. 837, 1969.
35. Korchynsky, M., Graham Research Laboratories, Jones and Laughlin Steel Corporation, Pittsburgh, Pennsylvania, personal communication to Dr. Clough.
36. Morrison, W. B., "The Effect of Grain Size on the Stress-Strain Relationship in Low Carbon Steel," Transactions ASM, Vol. 59, pp. 824, 1966.
37. Dieter, G. E., Jr., Mechanical Metallurgy, McGraw-Hill Book Company, New York, 1961.
38. Gladman, T., B. Holmes, and F. B. Pickering, "Work Hardening of Low Carbon Steels," Journal of the Iron and Steel Institute, Vol. 208, pp. 172, 1970.
39. Republic Steel Corporation, High Strength Low Alloy Steels, Cleveland, Ohio, 1972.

40. Underwood, E. E., Quantitative Stereology, Addison-Wesley Publishing Company, Reading, Massachusetts, 1970.